Alma Mater Studiorum – Università di Bologna

DOTTORATO DI RICERCA IN

ONCOLOGIA E PATOLOGIA SPERIMENTALE

Ciclo XXVIII

Settore Concorsuale: 06/D3

Settore Scientifico disciplinare: MED/06

Possibile Ruolo Chemopreventivo Dell'Acido Eicosapentaenoico Sul Cancro Colorettale Insorto Su Colite

Presentata da: dott.ssa Chiara Fazio

Relatore:
Prof. Lorenzo Montanaro

Coordinatore Dottorato:
Prof. Pier Luigi Lollini

Correlatori:
Prof. Massimo Derenzini
Prof. Luigi Ricciardiello

Esame finale anno 2016

TABLE OF CONTENTS

LIST OF FIGURES

LIST OF TABLES

LIST OF ABBREVIATIONS

ACF	Aberrant Cript Foci
ADAM	A Disintegrin And Metalloproteinase
AFAP	Attenuated FAP
AID	Activation-Induced Cytidine Deaminase
ALA	Alpha-linolenic acid
ANOVA	Analyses Of Variances
AOM	Azoxymethane
APC	Adenomatous Polyposis Coli
ARA	Arachidonic Acid
ATOH1	Atonal homolog 1
BSA	Bovine Serum Albumin
CAC	Colitis Associated Colorectal Cancer
C-CSF	Granulocyte colony-stimulating factor
CD-14	Cluster of differentiation 14
CD	Crohn Disease
CDH1	Cadherin 1
CGI	CpG island
CIMP	CpG island methylator phenotype
CIN	Chromosomal instability
CM	Conditioned Medium
COMB	Combination
COX-2	Cyclooxygenase

CpG	Cytosine phosphate Guanine
CRC	Colorectal Cancer
CRI	Cancer Related Inflammation
CSL	CBF1, Suppressor of Hairless, Lag-1
CTRL	Control
CVDs	Cardiovascular diseases
CXCL8	Chemokine-8
DC	Dendritic Cells
DHA	Docosahexaenoic Acid
DMSO	Dymethyl Sulfoxide
DNA	Deoxyribonucleic acid
DPA	Docosapentaenoic acid
DSB	Doublestrand Break
DSS	Dextran sodium sulfate
ECM	Extracellular Matrix
EGF	Epidermal growth factor
EMT	Epithelial to Mesenchymal Transition
EPA	Eicosapentaenoic Acid
EPA-FFA	Eicosapentaenoic Acid-Free Fatty Acid
FACS	Fluorescence Activated Cell Sorting
FAP	Familial adenomatous polyposis
FBS	Fetal Bovine Serum
FO	Fish Oil
GAPDH	Glyceraldehyde 3-phosphate dehydrogenase
GC-MS	Gas Cromatography-Mass Spectrometry

GM-CSF	Granulocyte macrophage colony-stimulating factor
Gp130	Glycoprotein 130
GPRs	G-Protein Receptor
HIF1α	Hypoxia-inducible factor 1 alpha
HNPCC	Hereditary nonpolyposis colorectal cancer
HR	Homologous Recombination
IBD	Inflammatory Bowel Disease
IFN-g	Interferon-γ
IKK.-α	IκB kinase
IL	Interleukin
IMDM	Iscove's Modified Dulbecco Media
JAG1	Jagged1
LOH	Loss of heterozygosity
LPS	Lipopolysaccharide
MCP-1	Monocyte chemoattractant protein-1
MIP1-β	Macrophage inflammatory protein 1-β
miRNA	Micro RNA
MMP9	Metalloprotease 9
MMPs	Metalloproteases
MMR	Mismatch repair system
MSI	Microsatellite instability
MSI-H	High-frequency MSI
NECD	Notch Extracellular Domain
NF-Kb	Nuclear Factor-Kappa B
NICD	Notch Extracellular Domain

NK	Natural Killer
NRARP	Notch1-regulated ankyrin repeat protein
O-fut1	O-fucosyltransferase 1
PBS	Phosphate buffered saline
PGs	Prostaglandins
PGE_2	Prostaglandin E2
PGE_2	Prostaglandin E3
PMA	Phorbol 12-myristate 13-acetate
qRT-PCR	Quantitive Real Time PCR
RIPA	Radioimmunoprecipitation assay buffer
RNA	Ribonucleic acid
ROS	Reactive Oxygen Species
RPMI	Roswell Park Memorial Institute
Rsv	Resolvin
SDS	Sodium dodecyl sulfate
SEM	Standard error of the mean
shRNA	Short hairpin RNA
siRNA	Small Interfearing RNA
Stat3	Signal Transducer Activator of Transcription-3
TGF-β	Transforming growth factor beta
TH1	T helper
Tregs	T-regulator cells
UC	Ulcerative Colitis
YAP	Yes-associated protein
ω-3 PUFAs	Omega-3 Polyunsatured Fatty Acids

ABSTRACT

The Notch1 signaling pathway has a pivotal role in cell fate regulation and has been found to be critically deranged in different cancers, including colorectal cancer (CRC). Inflammation is known to play an important role in the pathogenesis of CRC and a prominent function of Notch1 during inflammation has been recently demonstrated. Epithelial to Mesenchymal Transition (EMT), a crucial process in the malignant transformation, is modulated by inflammation and Metalloproteinase-9 (MMP9) is involved in this interaction. Eicosapentaenoic Acid is an omega-3 polyunsaturated fatty acid (ω-3 PUFA) known for its anti-inflammatory properties as well as for its capability in preventing colon cancer development both in sporadic and in hereditary settings. In particular, our group has demonstrated that an extra-pure formulation of Eicosapentaenoic Acid as the free fatty acid (EPA-FFA) protects from CRC development in a mouse model of colitis-associated cancer (CAC) by modulating the Notch signaling pathway. In the present work, we re-created an *in vitro* model of inflammatory-driven CRC by exposing colon cancer cells to a cytokine-enriched conditioned medium (CM) obtained from THP-1-differentiated macrophages. We found, for the first time, that CM strongly induces Notch1 signaling and EMT markers, increasing the capability of cells to invade. Importantly we found that, upon CM exposure, Notch1 signaling is dependent on MMP9 expression. Finally, we show that a non-cytotoxic pre-treatment with 50 μM of EPA-FFA for 72h counteracts the effect of inflammation on Notch1 signaling and EMT, leading to a reduction of invasiveness. Taken together, our data demonstrate that in CRC inflammation up-regulates Notch1 signaling through MMP9 and that this mechanism can be effectively counteracted by EPA-FFA.

1. INTRODUCTION

1.1 Colorectal Cancer (CRC)

Colorectal cancer (CRC) is a malignant transformation that affects the first and the final sections of the large intestine, namely the colon and the rectum (1). CRC represents the third most common type of cancer and the fourth leading cause of cancer-related death worldwide, with more than a million of newly diagnosed cases every year (2). The majority of colorectal cancers (85-90%) occurs sporadically, actually without a clearly recognizable predisposition, while a smaller percentage of cases is attributable to familial or hereditary forms (2-5%) or to the persistence of inflammatory conditions (1-2 %), (Figure 1), (3). An important non-modifiable risk factor for CRC is represented by the increasing age: more than 90% of the new cases are diagnosed among people aged 55 years or more (4). Importantly, many CRC risk factors are modifiable factors connected to the dietary habits (i.e. obesity), smoking or alcohol consumption (5). The high incidence of the sporadic form of CRC outlines the substantial effect of the environment on the pathogenesis (6). Indeed, the probability to develop CRC changes in relation to the geographical distribution: the highest incidence is found in economically developed countries, in particular Australia/New Zealand, United States and Europe, while the lower incidence is found in Africa and South-Central Asia (Figure 2), (3).

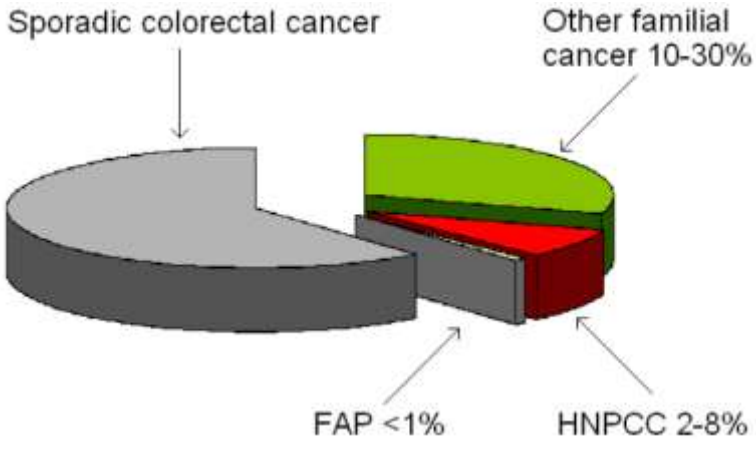

Figure 1: Subtypes of Colorectal Cancer. FAP= familial adenomatous polyposis; HNPCC = hereditary non-polyposis colorectal cancer. Modified from Bart 2000, (7).

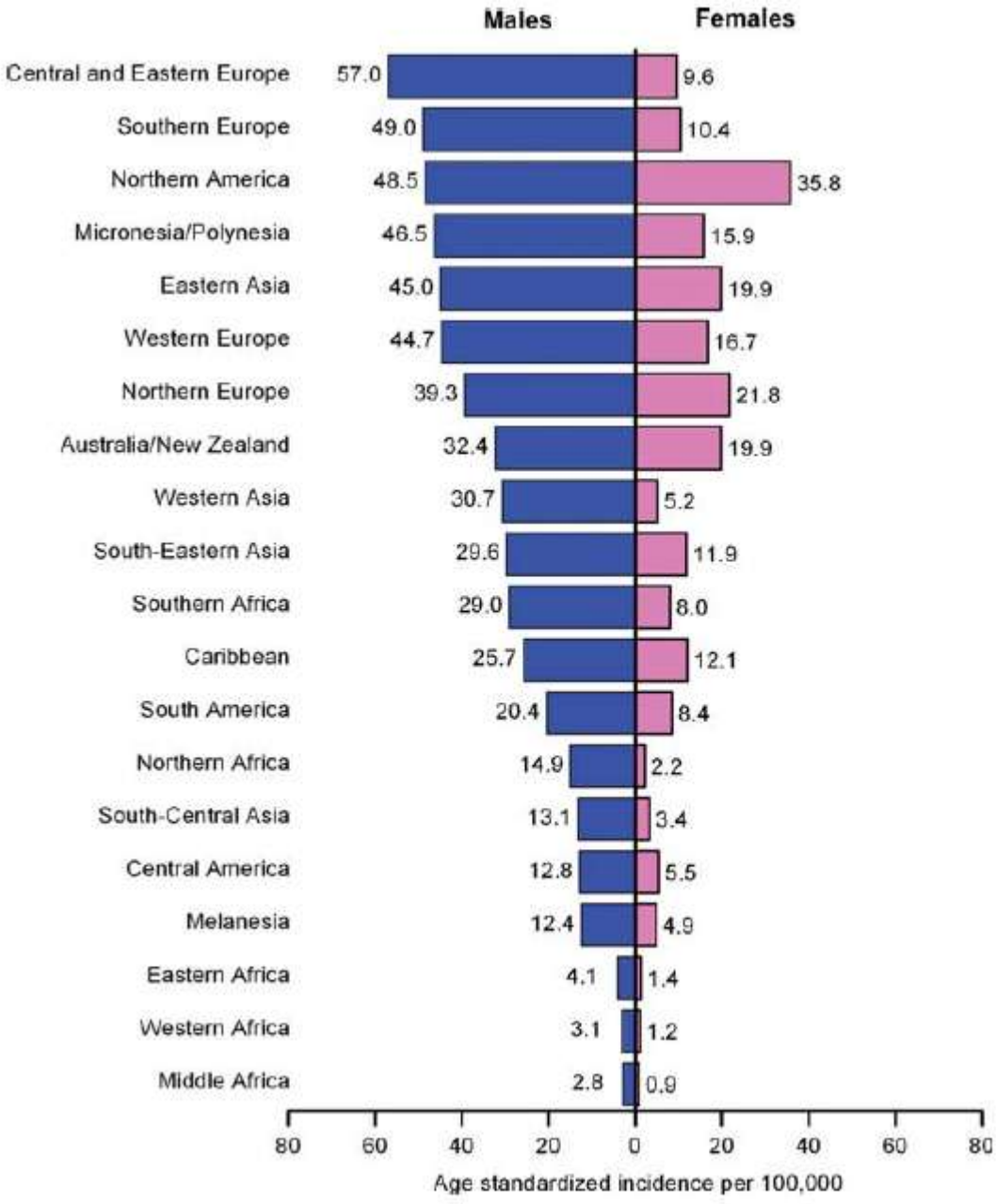

Figure 2: Age-Standardized Colorectal Cancer Incidence Rates by Sex and World Area. From GLOBOCAN 2008, (3).

1.1.1 Colorectal carcinogenesis

The gut epithelium is a highly proliferative organ, with a substantial cellular turnover. Homeostasis is achieved by a fine balance among cellular proliferation, differentiation and death (8). The colorectal carcinogenesis arises from a disruption of this delicate balance. In particular, the interplay between environmental factors and susceptibility genes sets off a complex series of neoplastic events. In 1990, Fearon and Vogelstein proposed a multistep adenoma-to-carcinoma model for colorectal tumorigenesis, based on the assumption that a cell must accumulate a specific sequence of genetic alterations in order to undergo full malignant transformation (9). Elevated rate of crypt fission, defined as aberrant crypt foci (ACF) is considered the first detectable defect in pre-neoplastic intestine by which microadenomas develop (10). Sustained by a pro-tumorigenic microenvironment, which promotes the acquisition of additional mutations, a small part of ACF can evolve toadenoma and then to colorectal carcinoma (Figure 3).

The genetic mutations crucial for the carcinogenic process affect fundamentally three types of genes: 1) proto-oncogenes 2) tumor suppressor genes 3) DNA repair genes (11). Proto-oncogenes, such as *K-RAS*, are activated into oncogenes even by a single "gain of function" mutation; this activation results in the capability for the cell to grow in the absence of growth factors but also in

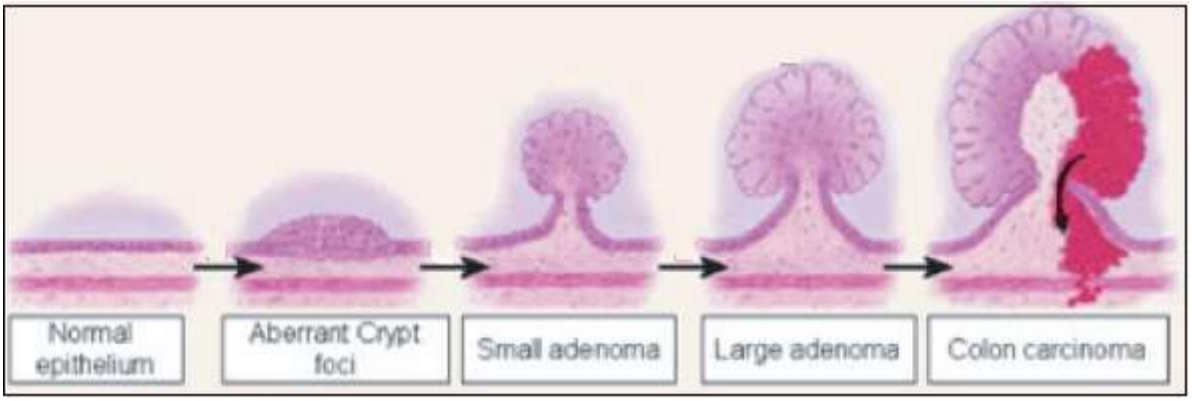

Figure 3: The Adenoma to Carcinoma sequence, modified from Guruswamy and Rao 2008, (12).

abnormal invasion capability and in the disruption of the apoptosis mechanism (13). Tumor suppressor genes, such as *APC* or *p53,* require two genetic events (one in each allele), for their inactivation resulting in a "loss of function". Finally, alterations in DNA repair genes, such as *SMAD4,* that normally preserve newly replicated DNA from errors by repairing mismatched bases in the molecule, result in an abnormal accumulation of mutations (14).

The Adenomatous Polyposis Coli *(APC)* is considered the driver gene in the pathogenesis of CRC and is mutated in approximately 85% of cases (15). APC controls the WNT/ β-catenin signaling pathway: inactivating mutations in APC lead to stabilization of β-catenin and nuclear translocation, which in turn leads to the transcription of downstream oncogenes such as CYCLIN-D1 and C-MYC (16).

In this context, the above-mentioned genetic events interact with epigenetic mechanisms, inducing the acceleration of the accumulation of mutations. The principal epigenetic mechanisms involved in the ethiopathogenesis of the CRC are: the chromosomal instability (CIN), the CpG island methylator phenotype (CIMP) and deficiency of genes of the DNA mismatch repair system (MMR), (17). CIN consists in an elevated frequencies of whole-chromosome missegregation that leads to chromosomal imbalance, namely aneuploidy, and is a predominant pathway in CRC since it occurs in 85% of the cases (18). The CIMP, which includes also sporadic microsatellite instability (MSI), represents the aberrant methylation of entire regions or CG sequences found in the promoter of genes, and is associated with the downregulation/loss of their expression; up to 15% of the cases of CRC present a CIMP phenotype (19). Then, the MMR pathway, tipically resulting from a germline mutation in the DNA of the mismatch repair (MMR) genes such as *MSH2*, *MLH1*, *MSH6* and *PMS2*, allows persistence of mismatch mutations all over the genome (20).

1.1.2 Sporadic Colorectal Cancer

Most CRC (70%) develop as sporadic cancers, since one or more precise involved genes are not identifiable. A colorectal epithelial cell generally requires about 20-40 years to transform into a

metastatic tumor cell (15). In the classic 'adenoma-carcinoma' model, mutations in APC gene or loss of chromosome 5q (which includes the APC gene) are an early event, followed by mutations in KRAS, which generally occur in the intermediate adenoma stage. Then, a later event occurring during the malignant transformation from adenoma to carcinoma *in situ* is the mutation or LOH of p53 gene or deletions of chromosome 17p (which includes the p53 gene), (21). After the molecular characterization of CRC proposed by Fearon and Vogelstein, in the following decades of research it has been demonstrated that only 6.6% of CRC tumors is characterized by concurrent mutations in APC, KRAS and p53, while 38% of tumors had mutations in only one of these three genes (13). These observations led to consider the development of CRC in a more complex view. Indeed, alterations in additional pathways, as well as epigenetic changes in cancer related genes and modulation of non-coding RNA importantly contribute to the malignant transformation (22).

1.1.3 Familial and Hereditary Colorectal Cancer

Epidemiological studies indicate that approximately 15% of CRC occur in inherited patterns (23). Typically, hereditary CRC occurs upon an inherited predisposition and are characterized by germ-line mutations which confer a major risk to develop CRC at an earlier age of onset respect to the sporadic forms (24). According to the presence or absence of polyposis, the hereditary forms of CRC are classified in two main categories: the polyposis syndromes and Lynch syndrome (previously known as hereditary nonpolyposis colorectal cancer or HNPCC), respectively. The polyposis syndromes are further categorized in familial adenomatous polyposis (FAP), attenuated FAP (AFAP), MUTYH-associated polyposis (MAP) and other rare hereditary syndromes such as Peutz-Jeghers syndrome, Cowden syndrome and juvenile polyposis or, recently discovered, syndromes associated to mutations in DNA polimerases POLE and POLD1(25), (26).

In 1991, germline mutations in *APC* were proved to directly cause FAP; FAP patients typically develop hundreds to thousands of benign colorectal tumors during their second and third decades of life, of which some progress to carcinomas with a high probability (27).

Differently from FAP, MAP is an autosomal recessive disease due biallelic mutations in MUTYH gene, encoding for a DNA glycolase implicated in the Base Excision Repair system (28).

Lynch syndrome is characterized by an early onset of CRC at a median age of 42, usually in the proximal colon. The defect in Lynch syndrome is an alteration of the above-mentioned DNA mismatch repair system (28).

1.1.4 Colitis-associated Colorectal Cancer (CAC)

Colitis-associated colorectal cancer (CAC) is a subtype of colorectal carcinoma occurring in patients with Inflammatory Bowel Disease (IBD), (29). IBD-associated colorectal neoplasia accounts for 1-2% of all CRCs, and the importance of this subset of CRC is due to the early age of onset (40-50 years), (30). Ulcerative colitis (UC) and Chron's disease (CD), which are the two main forms of IBD, confer an increased risk to develop CAC in the successive 20 years after the first diagnosis, with a more convincent correlation for UC (31), (32). Although sporadic CRC and CAC share several molecular mechanisms and both require accumulation of mutations for cancer development, important pathogenic differences discriminate these two types of CRC. Importantly, in the case of CAC the classical ‘'adenoma-carcinoma’ sequence is substituted by the 'inflammation-dysplasia-carcinoma' sequence, in which the tumor formation derive from a flat and nonpolypoid dysplasia, frequently appearing as a multifocal condition with the involvement of a larger area of the colon (31); in this context, the molecular events that underlie the tumorigenesis are only in part shared by sporadic CRC and CAC. On an hand, the genomic instability in CIN and MSI occurs approximately at the same rate in both types of CRC. Gene silencing by CpG island (CGI) hypermethylation also occurs in both sporadic CRC and CAC (33). On the contrary, the temporal sequence of genetic mutations results opposite between sporadic CRC and CAC: the loss of APC function is usually a rare and a late event in IBD-associated neoplasia intervening in the shift from dysplasia to CAC, differently from sporadic CRC (34). Moreover, while p53 alterations characterize the final steps of the multistage process of sporadic carcinogenesis, in CAC, p53

inactivation occur early and is sometimes observed in absence of dysplasia or in presence of indefinite dysplasia, indicating that it can be induced by a chronic inflammatory state preceding the onset of CRC (35). Notably, an age-related hypermethylation is found in precancerous colonic lesions of patients with IBD, although the global CGI methylation pattern in CAC is also influenced by the CIMP status (36). In addition, hypermethylation of hMLH1 promoter gene was detected in CAC characterized by a high-frequency MSI (MSI-H) inducing a defective DNA mismatch repair system (37).

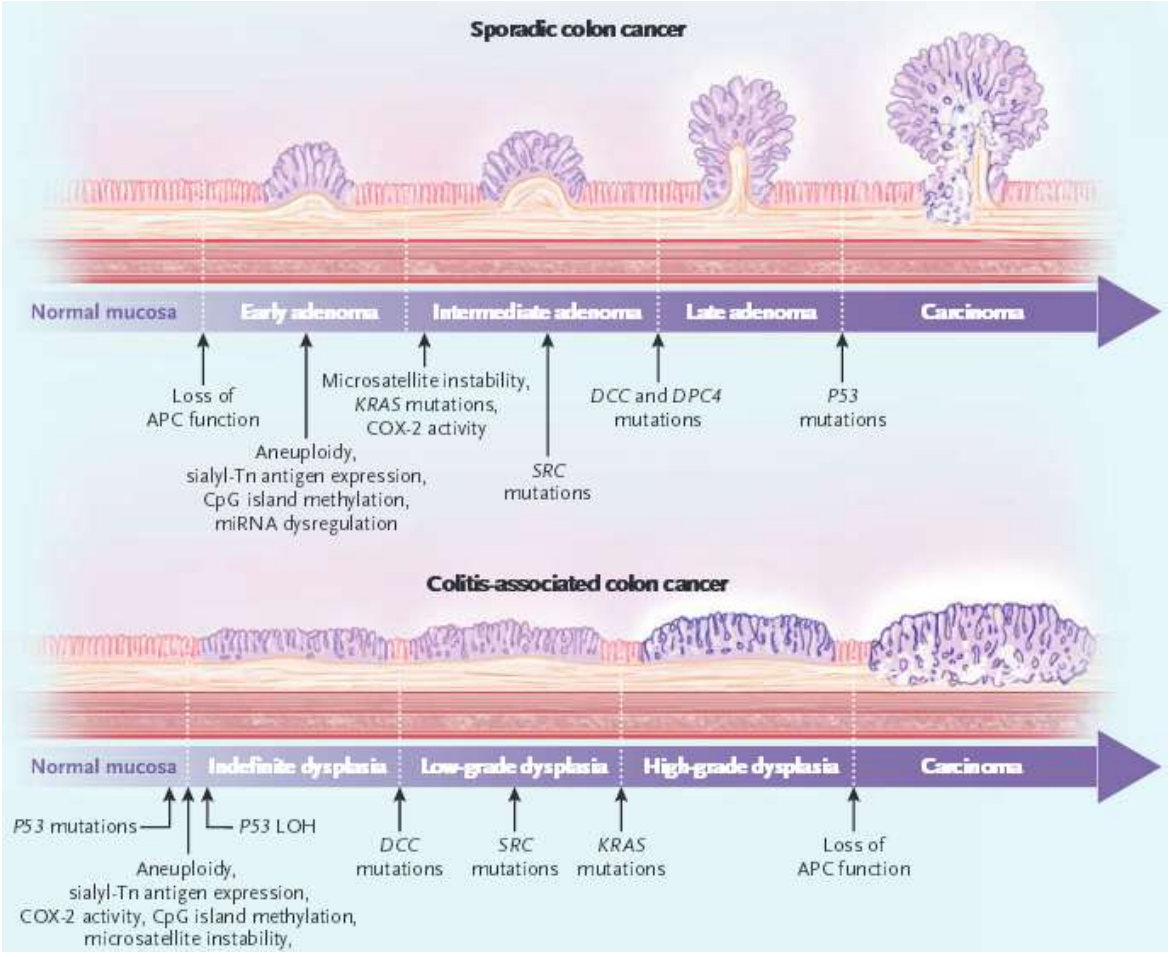

Figure 4: Differences in molecular pathways involved in CRC and CAC development, from Beaugerie 2015, (38).

1.2 Cancer-related inflammation (CRI)

CAC represents one of the clearest evidence of the connection between inflammation and cancer. In the case of CAC, the long standing inflammation contributes to the onset of cancer (39). However, besides IBD, chronic exposure of intestinal epithelial cells to pro-inflammatory *stimuli* can be due to heterogeneous reasons, including infections (40), microbiota alterations (41), metabolic disorders and obesity (42). These evidences suggest that inflammation is implicated in many different molecular events, delineating a complicated network linking inflammation to cancer. In this context, the role of inflammation is still not fully understood, even if the first characterization of leucocytes in tumor samples by Virchow date back more than one century ago (43).

In sporadic CRC, as well as in the majority of solid tumors, epithelial cells are surrounded by an inflammatory microenvironment highly populated by immune cells and rich in inflammatory mediators (44). This inflammatory *milieu* within the tumor microenvironment represents the "cancer-related inflammation" (CRI) that is now considered one of the hallmarks of cancer (44), (45).

The inflammatory tumor microenvironment is represented by a various mixture of cellular subtypes -CD4(+) T-helper 1 (T(H)1) cells, CD8(+) cytotoxic T cells myeloid cells, T regulatory cells (Tregs), T-helper interleukin (IL)-17-producing (T(H)17) cells, leukocytes, only to cite some- and their products, namely the pro-inflammatory mediators -such as cytokines, chemokines, growth factors, proteases and immunosuppressive molecules (29). Notably, the pro-inflammatory mediators can be also be produced by the cancer cells in response to the microenvironmental *stimulus* (Figure 5) (46),(47): from one part this can represent an ongoing anti-tumor response of the organism, from the other part it can be a sign of immune system subversion by the tumor for its

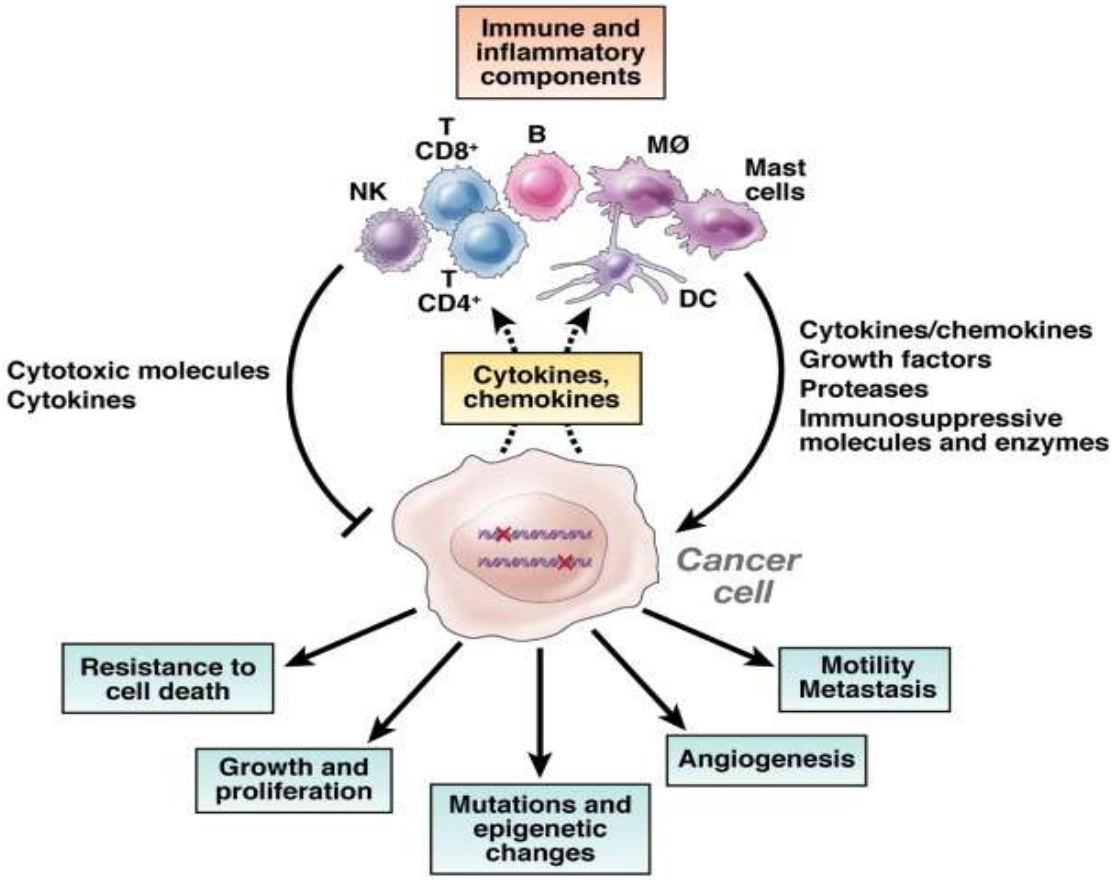

Figure 5: The link between cancer and inflammation, from Grivennikov 2010, (48).

own benefit. Indeed, the CRI can play a decisive role not only in the initiation of malignant transformation, but also in other mechanisms concerning the tumor progression, such as proliferation and survival of malignant cells, angiogenesis, metastasis and subversion of adaptive immunity.These mechanisms involve transcription factors such as Nuclear Factor-kappaB (NF-κB) and Signal Transducer Activator of Transcription-3 (Stat3), (49) and are driven by different pro-inflammatory components, such as Interleukin (IL)-1β, IL-6 and Tumor Necrosis Factor (TNF)-α (50). It has been demonstrated that the above-mentioned cytokines are able to affect multiple steps of the CRI cascade in the context of both CAC and CRC (43). Similarly, Chemokine-8 (CXCL8) has been also studied for its primary role in the pathogenesis of sporadic CRC (51), (52), (53). In particular, one of the proposed mechanisms at the basis of the pro-tumorigenic role of ongoing

inflammation is that epithelial cells can produce reactive oxygen and nitrogen intermediates in response to the stimulus of the cytokines, which lead to DNA damage and, consequently, gene mutations and epigenetic alterations (Figure 6). Moreover, inflammatory mediators downregulate DNA repair pathways by a variety of mechanisms, such as the hypoxia inducible factor (HIF)-1α, the Activation-Induced Cytidine Deaminase (AID); the doublestrand Break (DSB), or the homologous recombination (HR), (44). These mechanisms can converge to the accumulation of microsatellite and chromosomal instabitlity, as shown in Figure 7.

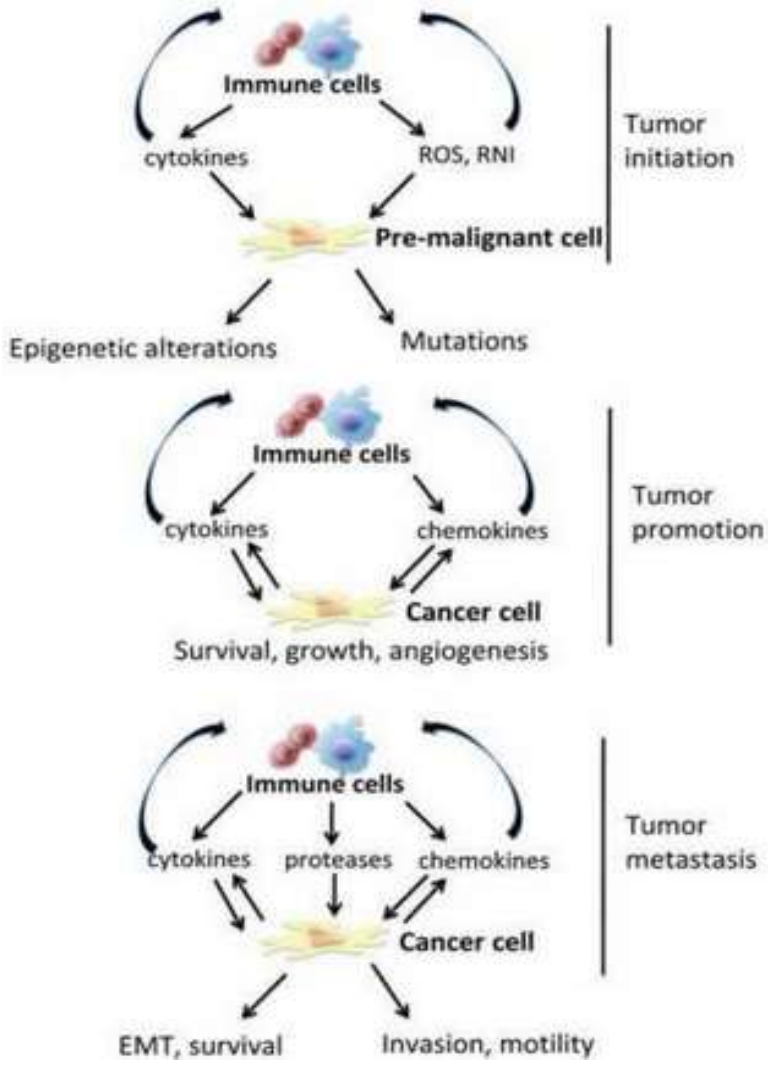

Figure 6: Molecular pathway involved in inflammation and oncogenesis, from Grivennikov 2010, (54).

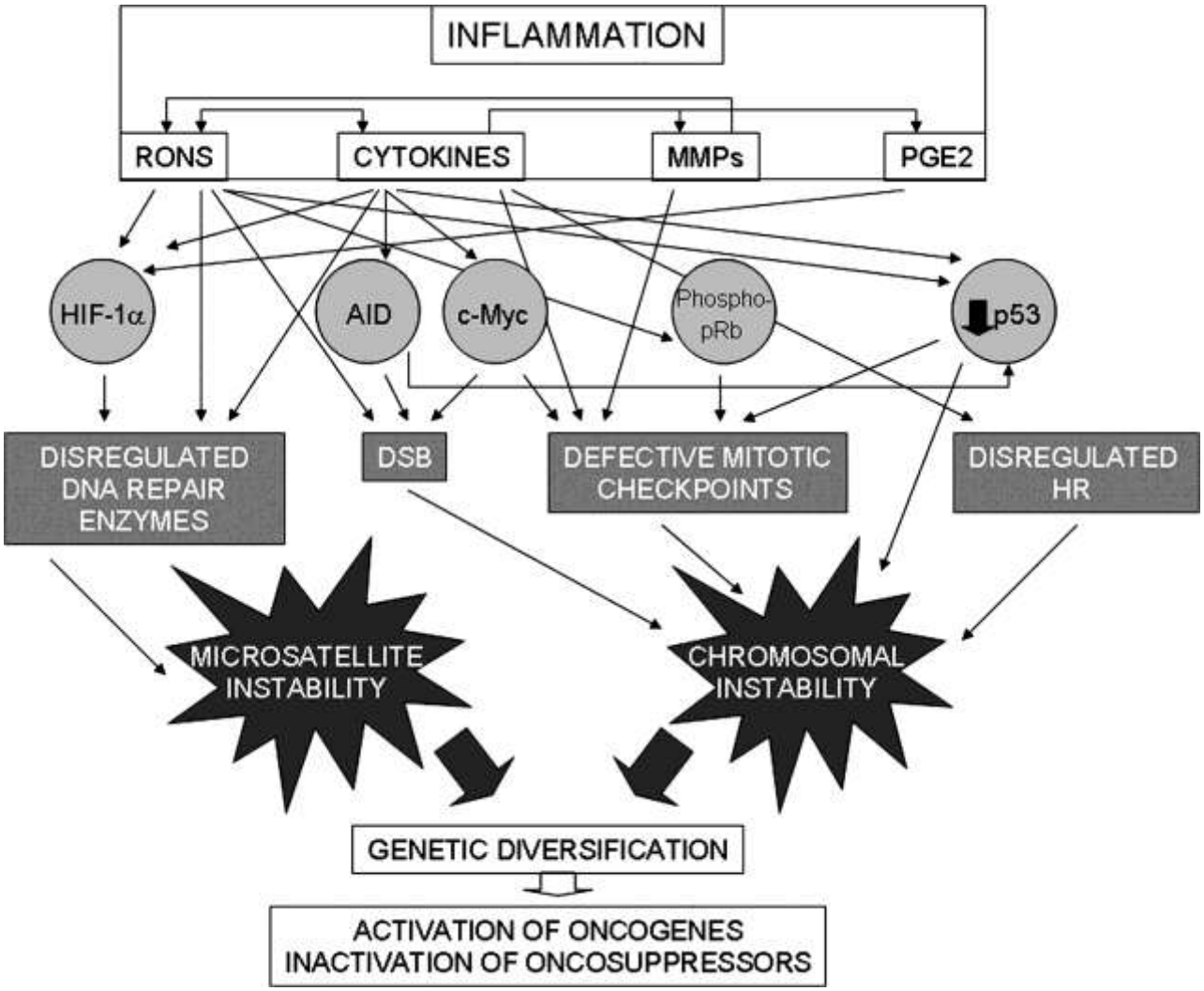

Figure 7: Molecular pathways linking CRI and genetic instability. From Colotta 2009, (44).

Due to the complexity of these interconnections, the effects of the combined pro-inflammatory mediators, resembling the inflammatory *milieu* within the tumor microenvironment, in the setting of cancer development and progression, particularly in sporadic CRC; have not been completely elucidated.

1.3 The Notch1 signaling

Notch1 signaling is a highly conserved molecular pathway which controls morphogenesis and organ formation in both vertebrate and invertebrates organisms (55), (56). Notch1 pathway can drive a surprisingly wide spectrum of specific functions, such as differentiation, proliferation and apoptosis, which are able to influence cell fate and to regulate the homeostasis of tissues (57). Due to its fundamental function, the involvement of deregulated Notch1 signaling in many pathological processes is understandable (58), as well as the possibility of considering it as a common cause for different types of tumors (59).

Although the functions mediated by the Notch1 signaling can be extremely complex, most of the Notch1-dependent processes are based on the same molecular mechanism, grounded on a direct cell-cell model of communication (60).

In humans, the core components of this pathway includes four distinct Notch1 receptors (Notch1-4) and their ligands (Jagged1, Jagged2, DLL1, DLL3 and DLL4). Both Notch1 receptors and ligands are single-pass trans-membrane proteins with extracellular domains characterized by multiple epidermal growth factor (EGF)-motifs. (49), (Figure 8).

The Notch1 receptors arise from a larger precursor of 300 KDa which need to be further processed in order to obtain the mature form. The first post-translational modification occurs in the endoplasmic reticulum and depends on the enzymatic activity of O-fucosyltransferase 1 (Ofut1); (61). Subsequently, the furin-like convertase enzyme carries out the cleavage of the glycosylated precursor in the Golgi, generating the N-terminal extracellular domain of Notch1 (NECD) and the transmembrane-Notch1 intracellular domain (NICD), which together constitute the mature receptor. This complex is further glycosylated during the passage through the Golgi by Fringe glycosyltransferase enzymes. Then, Notch1 mature receptors are translocated on the cellular membrane (62).

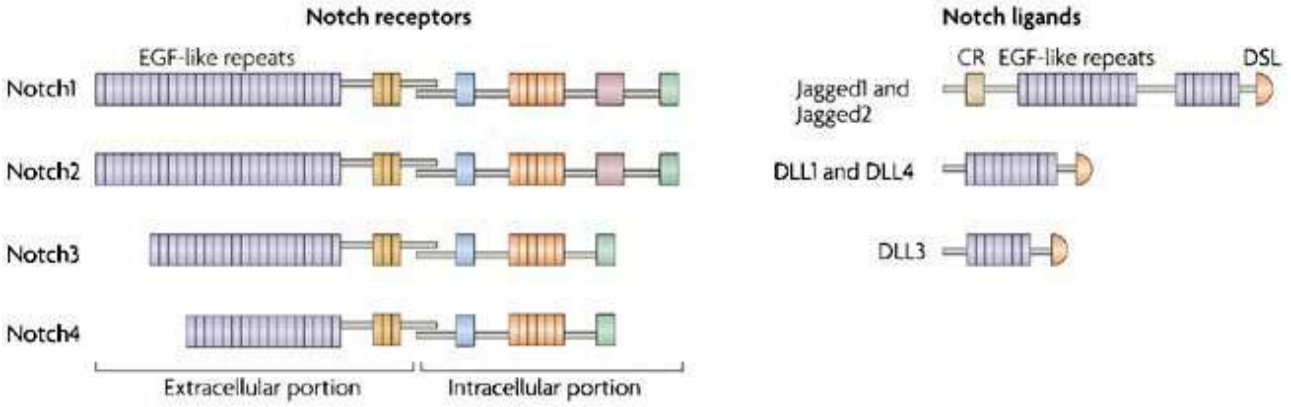

Figure 8: The Notch1 receptors and Ligands, modified from Andersson 2011, (58).

The physical interaction of Notch1 receptors with one of the specific ligands activates the signaling and Notch1 receptors undergo subsequent proteolytic cleavages. The first proteolityc event is catalyzed by the TACE metalloproteinase (ADAM17) and induces the cleavage of the extracellular portion of the receptor (NECD) which is subsequently internalized through endocytosis (63). The remaining anchored part of the receptor is further processed by the γ-secretase enzyme releasing the active intracellular domain of Notch1 (NICD).

In the canonical Notch1 signaling, NICD translocates into the nucleus where interacts with the transcriptional repressor protein CSL/RBP-J. Following the recruitment of co-activators Mastermind-like (MAML) and the histone acetyltransferase (HAT) p300, CSL/RBP-J is converted into a transcriptional activator, inducing the transcription of downstream target genes including Hes1 and c-Myc (64), (Figure 9).

Importantly, recent literature acknowledges an RBP-Jκ-independent activation of the Notch1 pathway, able to participate in several cellular processes, which is defined the "non-canonical Notch1 pathway" (65). In particular, a role for non-canonical Notch1 signaling in oncogenesis has been suggested by the evidence that inhibition of γ-secretase does not block all Notch1-related

functions in tumor cells (66). The mechanisms able to interact in a non-canonical manner with Notch1 are involved in the regulation of the Wnt signaling pathway, affecting the stability of β-catenin (67) , as well as in the response to inflammation, as reported below.

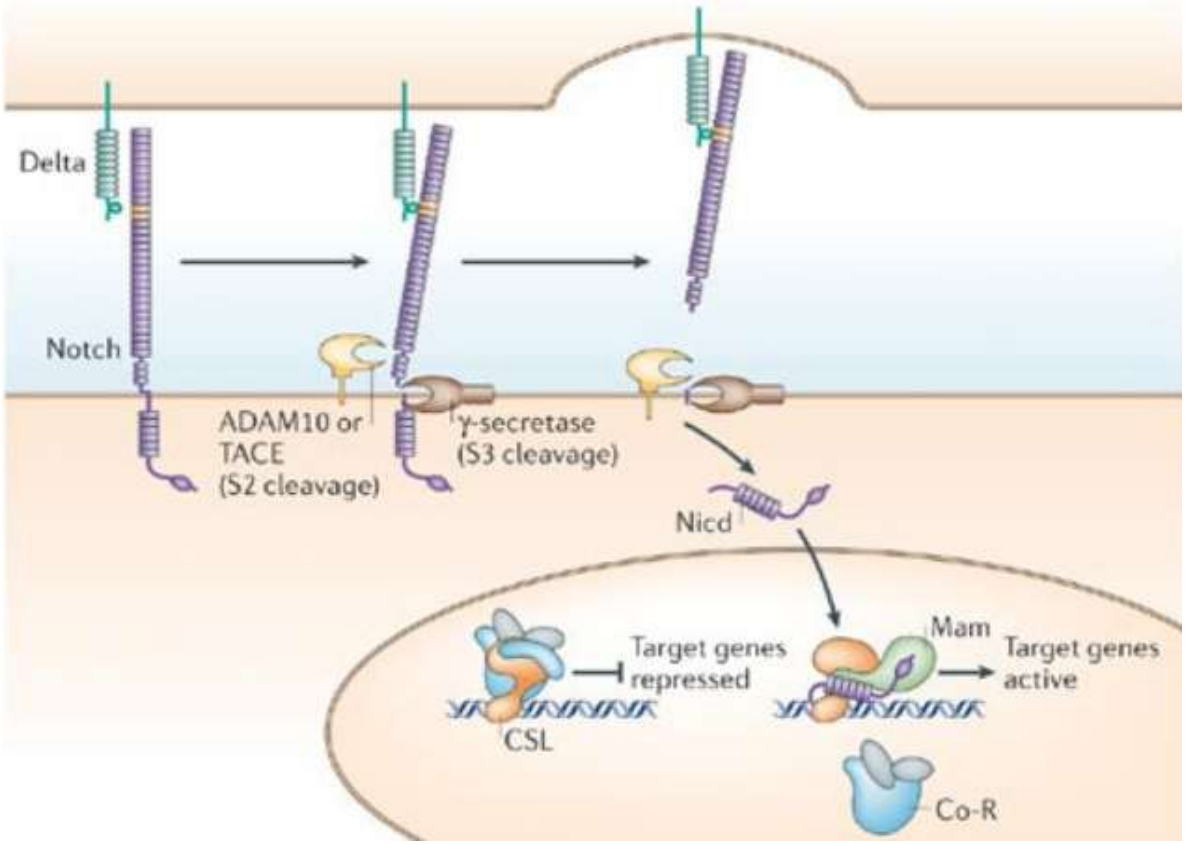

Figure 9: The Notch1 pathway. From Bray 2006, (56).

1.3.1 Notch1 signaling in CRC

In physiological conditions, Notch1 signaling is crucial for the maintenance of stem cell phenotype as well as for the regulation of cell fate in the intestinal tissue (68). However, it is well known that the deregulation of the Notch1 signaling cascade plays a pivotal role in several solid tumors, including CRC (69).

Importantly, while DLL1-mediated Notch1 signaling is required for intestinal stem-cell homeostasis (70), the binding to Jagged1 is associated with colon carcinogenesis (71). It has been recently demonstrated that besides the classical downstream target *HES1*, which in turn blocks atonal homolog 1 (*ATOH1*) transcription, in the gut epithelium the Notch1-regulated ankyrin repeat protein (NRARP) transcription level accurately reveals the intestinal activation of Notch1 (72).

Depending on the CRC setting, a dichotomy for the role of Notch1 pathway activation has been reported: while in sporadic or hereditary models of CRC Notch1 seems to act as an oncogene and is required for adenoma formation (73) and cancer progression (74), in CAC Notch1 seems to have a tumor suppressor role and its inhibition is associated with increased apoptosis (75). The tumor-suppressor role of Notch1 in the development of CRC has been strongly demonstrated by Kim and colleagues, which showed that the induced activation of Notch1 in a transgenic murine model of FAP (ApcMin/+ mouse model) converted intestinal high-grade adenoma into low-grade adenoma (72).

1.3.2 Notch1 signaling and inflammation

Recent experimental results acknowledge the role of the Notch1 pathway for regulating inflammatory processes (76). Moreover, different pathways, involved in the response to inflammation, are able to modulate the non-canonical Notch1 pathway, such as the nuclear factor kappa-light-chain-enhancer of activated B cells (NFkB) (77), the pathway of hypoxia-inducible factor 1 alpha (HIF- 1α) (78), the epithelial-to-mesenchymal transition (EMT), (79), (80), which is discussed below, the Wnt signaling (67) or the mitogen-activated protein kinase (MAPK) and nutrient sensor kinase mTOR (81), only to cite some.

In CRC, the activation of Notch1 signaling in response to pro-inflammatory *stimuli* has recently emerged (82). Taniguchi and colleagues showed that gp130, a co-receptor for IL-6, triggers activation of Yes-associated protein (YAP) and Notch1, independently of the classic gp130 effector

STAT3, leading to the proliferation of epithelial cell (83). Also, the protective role of Notch1 activation in the context of CAC tumorigenesis regards the role of Matrix Metalloproteinases-9 (MMP9), a protein involved in the epithelial to mesenchymal transition. Indeed, Garg and colleagues demonstrated that MMP9, despite notoriously being a pro-inflammatory mediator, plays a protective role by modulating Notch1 and β-catenin through p21 expression in a model of CAC (80). At the same time, it has been also demonstrated that MMP9 is able to induce an oncogenic activation of Notch1 signaling pathway in an inflammation-related context; indeed, Pope and his group recently found that the up-regulation of Claudin-1, an integral component of the tight junctions structure, causes the activation of Notch1-signaling through MMP9 and p-ERK, thus increasing the susceptibility to mucosal inflammation (84). Moreover, Lin J and colleagues sustain the role of inflammatory factors in promoting Notch1 pathway activation and colon cancer progression, for example through the axis IL-6/Notch1 (82).

1.4 Epithelial to Mesenchymal Transition (EMT)

Epithelial to mesenchymal transition (EMT) is a functional process recognized as a central feature of normal development. Several processes involved in embryogenesis, such as gastrulation, neural crest formation and heart morphogenesis, are grounded on the plastic transition between epithelium and mesenchyme (85). Through the EMT program, a polarized epithelial cell, normally interacting with the basement membrane via its basal surface, is subjected to various biochemical changes and acquires augmented migratory capacity, elevated resistance to apoptosis and increased production of extracellular matrix (ECM) components, globally assuming a mesenchymal phenotype (Figure 10), (86).

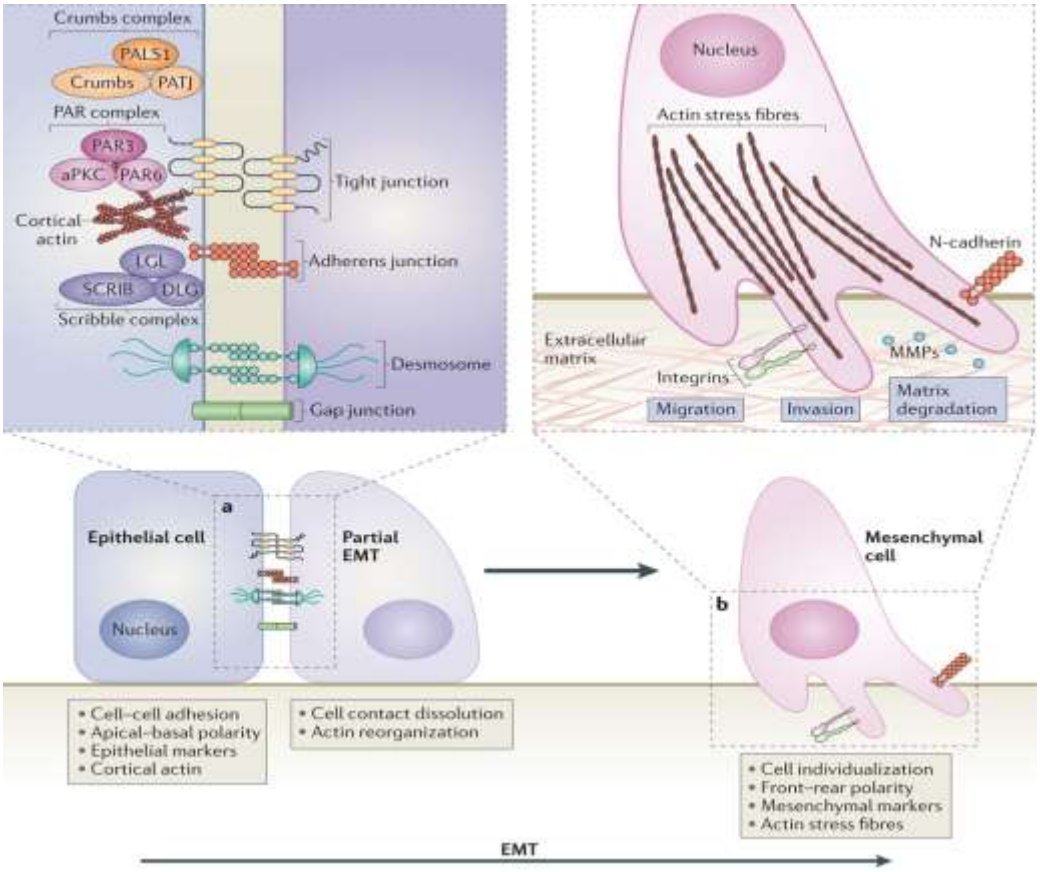

Figure 10: The epithelial to mesenchymal transition. From Lamouille 2014, (87).

Several molecular features characterized the EMT process, as summarized in Figure 11 (87).

During EMT, E-cadherin (encoded by CDH1 gene), a cell adhesion molecule of the membrane of most normal epithelial cells, is repressed or degraded. A variety of signal transduction pathways participate to the regulation of E-cadherin, among these SNAIL is known to repress CDH1(88). The family of SNAIL proteins (SNAIL1 and SNAIL2/SLUG) plays an important role during EMT: its function is to repress epithelial genes by binding to E-box DNA sequences through their carboxy-terminal zinc-finger domains (89). Then, homodimeric and heterodimeric basic helix–loop–helix (bHLH) transcription factors function as master regulators of lineage specification and differentiation. In particular, E12 and E47, TWIST1 and TWIST2 have key roles in EMT progression; the ZEB transcription factors (ZEB1 and ZEB2) also bind regulatory gene sequences at E-boxes and can modulate transcription (90). Notably, changes to the integrins during EMT also induces the expression of proteases, in particular of the matrix metalloproteinases (MMP) 2 and 9; this event leads to the degradation of the components of ECM protein and, subsequently, to an increased invasiveness. Moreover, MMPs are able to modulate the expression of specific transmembrane proteins involved in the release of the extracellular domain of E-cadherin, an event related to the loss of adherens junctions (91).

Besides these "classically" recognized master regulators of EMT, it has been recently demonstrated that many other signaling networks are involved in this process, such as miRNAs, TGFβ family proteins, the tyrosine kinase receptors, the insulin-like growth factor 1, only to cite some (87). Of particular interest for the present study is the evidence that Notch1, as well as inflammatory mediators, contribute to the induction of EMT. For instance, it has been reported that Notch1 signaling is required for EMT during endocardial cushion formation, and reduced SNAIL1 occurs in Notch1-deficient mice (92). Also, the release of IL-6 promotes EMT of breast cancer cells in culture, which correlates with a decrease in E-cadherin levels, an increase in SNAIL1 and TWIST

levels, leading to augmented cell invasion (93). Similarly, it has been demonstrated that the promotion of the EMT correlates with the increased secretion of IL-8 in tumor cells, and this latter in turn maintains the mesenchymal phenotype of the cells (94).

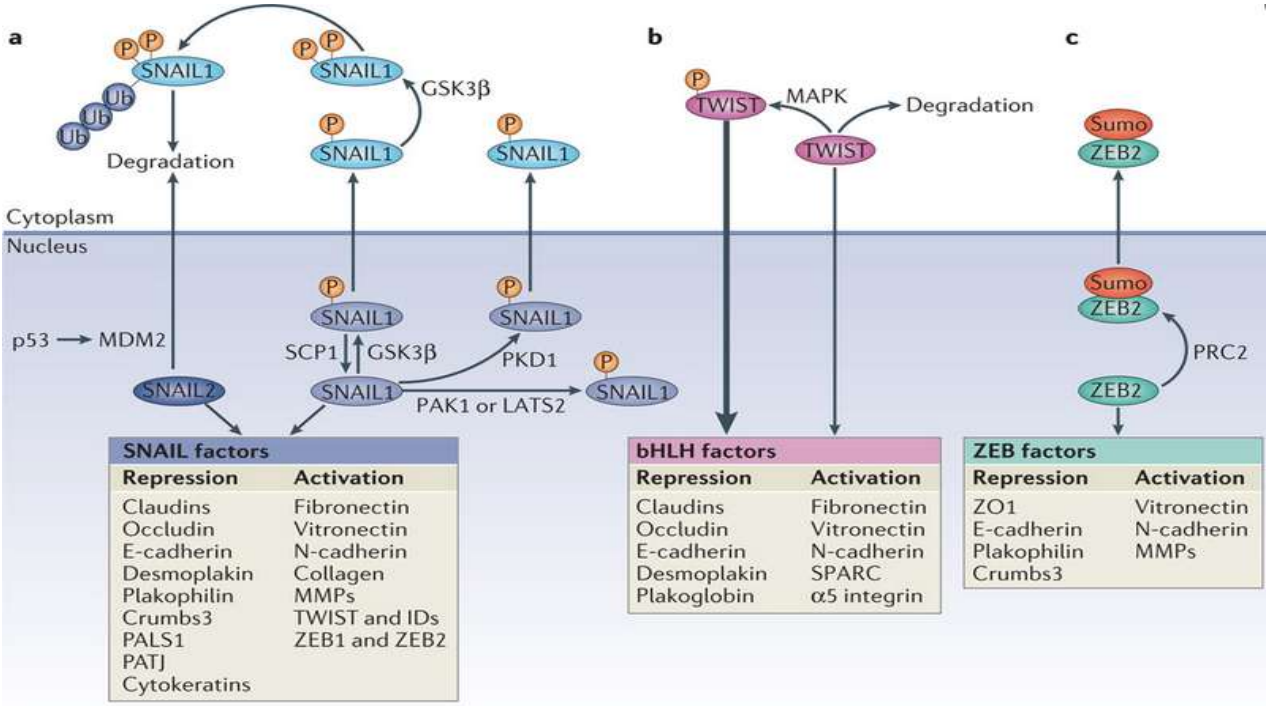

Figure 11: Transcriptional factors involved in EMT. From Lamouille 2014, (87).

1.4.1 Epithelial to Mesenchymal Transition in CRC

EMT has been well documented in multiple cancer models, including CRC (95). During tumorigenesis, EMT increases the motility and invasiveness of cancer cells; in parallel, malignant transformation may be associated with signaling pathways promoting EMT (96), (97). Various processes associated with EMT occur during tumor progression, and these processes closely resemble those occurring in normal development. In this context, it is believable that a possible link between Notch1 signaling, inflammation and MMP9 could exist, even if the relationship among them remains unclear.

1.5 Polyunsaturated Fatty Acids (PUFAs)

The omega-3 Polyunsaturated Fatty Acids (ω-3 PUFAs) are carboxylic acids consisting of a long hydrocarbon chain with a carboxylic (-COOH) and a methyl group (-CH_3) located at the ends of the molecule. The nomenclature "ω-n" indicates the presence of double bonds at the n carbon of the hydrocarbon chain from the methyl group (Figure12).

Given their importance for human health ω-3 PUFAs are classified as essential fatty acids (98). Moreover, the ω-3 PUFAs are considered crucial dietary components because humans are not able to synthesize them from the precursor alpha-linolenic acid (ALA), despite they are fundamental constituents of cellular membranes. The ω-3 PUFAs include two subtypes of molecules: Eicosapentaenoic acid (EPA) and Docosahexaenoic Acid (DHA). EPA and DHA are present in fishes fed with algae (tuna, salmon, mackerel or sardines), able to produce them as result of their metabolism; however, a modest amount of PUFAs is also contained in plants (linseed, primrose, echium) but the bioavailability in this case is lower than the content in Fish Oil (FO), (99).

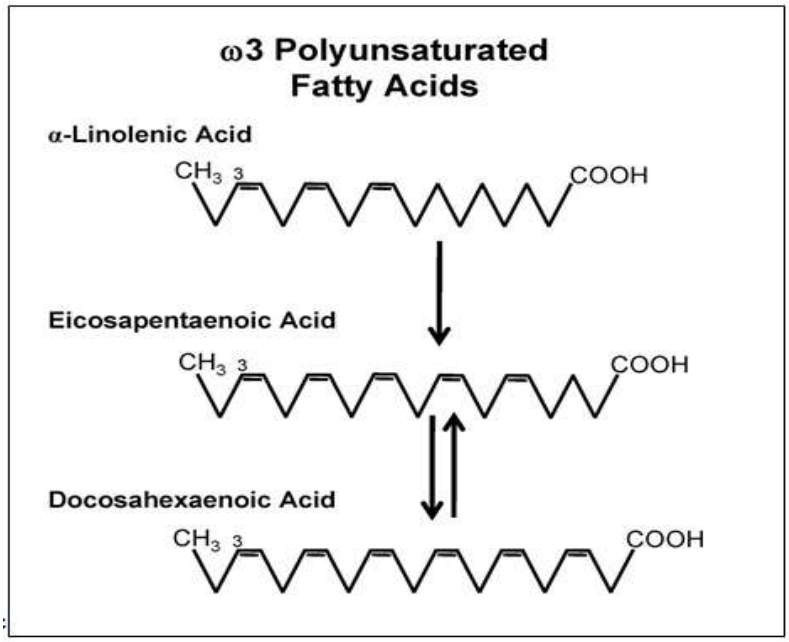

Figure 12: Structure of the Polyunsaturated fatty acids, from Rennison 2009 (100).

The healthy benefits related to the consumption of ω-3 PUFAs are largely proved by scientific literature: epidemiological studies began in 1970s and showed that the Greenland Eskimos had low mortality rates due to coronary heart disease because of their high consumption of ω-3 FO fatty acids. These epidemiological associations led to evaluate the preventive effects of FO against cardiovascular diseases (CVDs) as well as against inflammatory-related disease and, more recently, also against cancer (101) **.**

1.5.1 Anti-inflammatory properties of omega-3 PUFAs

Many data have been collected on the anti-inflammatory activity of EPA and DHA (102).

One of the key mechanisms of ω-3 PUFAs anti-inflammatory activity is the inhibition of COX-2-dependent synthesis of prostaglandins (PGs), through the replacement of Arachidonic acid –which is the substrate for the synthesis of the pro-inflammatory PGE2- from the cellular membrane by the ω-3 PUFAs. Therefore, by acting as an alternative substrate for COX-2, EPA and DHA lead to a reduction of PGE2 formation favoring the PGE3 series, which have anti-tumorigenic activity (103).

EPA is also able to generate oxygenated compounds such as Resolvins (Rvs), which are anti-inflammatory lipid mediators (104): in Fat-1 transgenic mice, which are able to convert endogenous ω-6 to ω-3 PUFAs, an increased tissue level of ω-3 led to a significant release of resolvins, with an effective reduction of inflammation and tissue injury in chemically induced colitis (105).

Moreover, ω-3 PUFAs are important modulator of the immune response. McMurray and colleagues showed that the PUFAs present in fish oil affects CD4+ T cell proliferation and cytokine production in C57BL/6 mice through the indirect suppression of T helper (Th) 1 cells by cross-regulation of enhanced Th2 activation (106)**.**

A further mechanism of action, particularly related to EPA action, could be exerted by the direct binding with G protein coupled receptors (GPRs), among which GPR120, a receptor present on the membrane of macrophages. Indeed, in the monocytic RAW264.7 cells and in primary

intraperitoneal macrophages, treatment with ω-3 PUFAs inhibited inflammation and enhanced systemic insulin sensitivity through GPR120 (107).

Nevertheless, the incorporation of EPA and DHA into the phospholipidic bilayer induces changes in the composition of the cellular membrane in terms of structure, fluidity and function of caveolae. Indeed, ω-3 PUFAs enrichment selectively modifies the cytoplasmic layer of detergent-resistant membrane domains, acting as functional rafts within the plasma membrane bilayer: this alteration could underlie the inhibition of T cell signal transduction (108).

1.5.2 Anti-neoplastic properties of omega-3 PUFAs on CRC

The beneficial effects of ω-3 PUFAs against CRC have been widely observed in many *in vitro* and *vivo* studies (109), (110), (111), (112).

Recently, our group found that a pure preparation of Eicosapentaenoic Acid as free fatty acid (EPA-FFA) led to a dramatic suppression of polyp number, load and size in the ApcMin/+ mouse model. Importantly, EPA-FFA fed animals displayed a significant reduction of COX-2 and nuclear β-catenin expression, and a significant decrease of lipid peroxidation (113).

We also demonstrated the effectiveness of substituting EPA-FFA for other dietary fats, in preventing inflammation and cancer in the AOM-DSS model of CAC. We found that EPA-FFA diet strongly decreased multiplicity, incidence and maximum size of tumor. Moreover EPA-FFA reduced cell proliferation and nuclear β-catenin expression and increased apoptosis. EPA-FFA treatment led to increased membrane switch from ω-6 to ω-3 PUFAs and a concomitant reduction in PGE2 production. Importantly, we found that EPA-FFA treatment restored the loss of Notch1 signaling found in the AOM-DSS control and resulted in the enrichment of Lactobacillus in the microbiota. These data suggest that EPA-FFA is an effective chemopreventive agent in CAC (114).

2. AIM OF THE WORK

Our group has recently demonstrated that an extra-pure formulation of Eicosapentaenoic Acid as Free Fatty Acid (EPA-FFA) is able to prevent cancer development both in the ApcMin/+ mouse model of FAP and in the AOM/DSS mouse model of colitis-associated cancer (CAC). However, the molecular mechanisms which underlie the chemopreventive role of EPA-FFA are poorly understood. Therefore, the aims of this study were:

- To re-create an *in vitro* model of interaction between a heterogeneous mix of proinflammatory mediators and CRC cells;
- To determine whether the Notch1 signaling is induced in this model and if this mechanism could be related to EMT in CRC cells;
- To investigate whether this pathway can be counteracted by the treatment with EPA in a free-fatty acid form (EPA-FFA).

3. MATERIALS & METHODS

3.1 Cell lines and treatments

The human colorectal cancer cell lines HT29 and HCT116, which represent two different molecular models of CRC, and the human monocyte cell line THP-1 were obtained from ATCC (Manassas, VA, USA; catalog numbers ATCC-HTB-38^{TM}, ATCC-CL-188^{TM}, ATCC-TIB-202^{TM}, respectively). In our laboratory, all cell lines are tested and authenticated every year using known genetic and epigenetic markers.

3.1.1 Cell lines Culture

HT29, HT29 Notch$^{-/-}$, HT29-MMP9$^{-/-}$ and THP-1 cell lines were cultured in Roswell Park Memorial Institute (RPMI)-1640 (with the addition of 50μM of β-mercaptoethanol for THP-1 and 2 μg/ml of puromycin for HT29 Notch$^{-/-}$), while HCT116 cell line was grown in Iscove's Modified Dulbecco Media (IMDM). The culture media were supplemented with 10% FBS (20% for THP-1), 100 U/ml penicillin, 100 μg/ml streptomycin and 2mM glutamine (Euroclone, Milan, Italy). The cells were maintained at 37°C and 5% CO2.

3.1.2 Treatment with Eicosapentaenoic Acid, free fatty acid (EPA-FFA)

Eicosapentaenoic acid as the free fatty acid (EPA-FFA, ALFA, SLA Pharma AG, Switzerland) was diluted 1:100 in EtOH 95% prior to use. This preparation was done freshly for every experiment protecting from light. EPA-FFA was used for cell culture treatments both at 72h and 14 days at the concentration of 50 μM. Every experiment was repeated at least three times.

3.1.3Treatment with Conditioned Medium (CM) or single pro-inflammatory mediators

HT29, HCT116 and LS174T cell lines were exposed to CM for 12h. In the case of EPA-FFA treated cells, after incubation with EPA-FFA for 72h the cells were washed with PBS and incubated with CM. HT29 cells were also incubated with 100 ng/ml of interleukin-6 (IL-6, Immunological Sciences, Roma, Italy), 1μg/ml of chemokine-8 (CXCL8, Sigma Aldrich) or 100 ng/ml of Tumor

Necrosis Factor-alpha (TNF-α, PeproTech Inc., Rocky Hill, United States), or their combination for 72h. Every experiment was repeated at least three times.

3.2 Conditioned Medium (CM) production and characterization

3.2.1 Conditioned Medium (CM) production

THP-1 cells were differentiated into macrophages using 5 ng/ml of phorbol 12-myristate 13-acetate (PMA, Sigma Aldrich, Milan, Italy) for 72h. After differentiation, the medium containing PMA was removed,THP-1 were washed with PBS and incubated in RPMI supplemented with 50 ng/ml of E.coli lipopolysaccharide (LPS, strain 055:B5, Sigma Aldrich) for 1h. Then, the medium containing LPS was replaced with fresh medium in order to obtain an LPS-free, cytokine-enriched conditioned medium (CM), (115), (116). After 24h, the CM was collected, filtered and stored at -80°C until use.

3.2.2 Fluorescence Activated Cell Sorting (FACS) analyses

The differentiation of THP1 into macrophages was assessed by determining the CD14 and CD11b positive cell population. Briefly, $0.5x10^6$ PMA-treated THP-1 cells were washed with PBS and suspended in 100ul of PBS supplemented with 1 % of Bovine Serum Albumin (BSA). Then, the samples were incubated with PerCP-conjugated anti-CD14 (Miltenyi Biotec, Bologna, Italy) alone, PE-conjugated anti-CD11b (Exalpha Biologicals, MA, U.S.A.) alone and with the combination of both antibodies on ice for 30 minutes. After antibody incubation, the cells were washed twice in 1 ml of PBS supplemented with 1 % BSA and resuspended in 300ul of PBS supplemented with 1 % BSA for further analysis with a FACSaria flow cytometer (BD Biosciences, Milano, Italy). Unstained cells were used as negative control. Data were analysed using BD FACSDiva software. The experiment was repeated at least twice.

3.2.3 Cytokine analysis

The CM composition was characterized by measuring the concentrations of the major cytokines: interleukin (IL)-1β, IL-2, IL-4, IL-6, CXCL8, IL-10, IL-12, IL-17, interferon-γ (IFNγ), monocyte

chemoattractant protein-1 (MCP-1), macrophage inflammatory protein 1-β (MIP1-β), tumor necrosis factor-α (TNFα), granulocyte-colony stimulating factor (G-CSF), granulocyte-macrophage colony-stimulating factor (GM-CSF) with a multiplex bead-based sandwich immunoassay (Bio-Plex, Bio-Rad Laboratories, Milan, Italy). This system relies on the emission of fluorescence resulting from the binding of a biotinylated antibody with a complex constituted by an antibody-coupled fluorescent dye bead and a specific cytokine. The reaction is revealed using streptavidin-phycoerythrin (streptavidin-PE), which binds to the biotinylated detection antibody. The Bio-Plex Manager™ software automatically calculates cytokines concentrations in the sample using a standard curve derived from a recombinant cytokine standard. The use of the different colour beads-set allows the discrimination and simultaneous quantification of multiple cytokines in the same sample. CM samples were also diluted with the specific Bio-Plex human sample diluent (1:10). 50 µl of cytokine standards or samples were added to each well of a 96-well plate and incubated with 50 µl of coupled beads for 30 minutes at room temperature under shaking conditions (850 rpm). Plates were then washed by vacuum filtration with 100 µl of Bio-Plex wash buffer three times, then 25 µl of diluted detection biotinylated antibody were added and plates were incubated for 30 minutes at room temperature undershaking conditions. After three filter washes, 50 µl of streptavidin-PE were added, and the plates were incubated for 10 minutes at room temperature under shaking conditions. Finally, plates were washed by vacuum filtration three times, beads were suspended in Bio-Plex assay buffer, and samples were analyzed on a Bio-Rad 96-well plate reader using the Bio-Plex Suspension Array System and Bio-Plex Manager software (Bio-Rad Laboratories, Hercules, CA). For each condition, two CM from different experiments were tested. Each sample was tested in duplicate, and cytokine standards supplied by the manufacturer were run on each plate.

3.3 Protein expression analysis

3.3.1 Protein extraction

Proteins were extracted from cultured cells with RIPA buffer (50 mM Tris-HCl-pH 7.4, 150 mM NaCl, 1% NP-40, Proteases and Phophatases inhibitors) and the total protein concentration was measured using the Lowry assay(Bio-Rad Laboratories), a colorimetric technique which allows to estimate the amount of proteins in biological samples.

First, proteins diluted tenfold in water were pre-treated with copper ion in alkalin solution for 20 minutes; then the aromatic amino acids in the treated sample reduced the acid present in the Folin Reagent further added. The final product of this reaction has a blue colour; the amount of proteins in the sample has been estimated reading the absorbance at 750 nm with a spectrophotometer (BIOMATE, ThermoSpectronic, MI, Italy) using a standard curve of a selected standard protein solution (in our case BSA solution).

3.3.2 Western Blotting

Eighty μg of proteins for each sample were separated on a 4-12% SDS-polyacrylamide gel (Life Technologies, Monza, Italy) and transferred o.n. onto nitrocellulose membrane. After being blocked with non-fat dry milk, the membranes were incubated overnight at +4°C with the following primary antibodies: mouse monoclonal anti-Notch1 1:1000 (clone mN1A, catalog number 629101, Biolegend, SA, USA), rabbit polyclonal anti-cleaved Notch1 1:500 (Val1744, catalog number 2421, Cell Signaling Technologies, Leiden, Netherlands), rabbit polyclonal anti-JAG1 1:200 (clone H-114, catalog number sc-8303, Santa Cruz Biotechnology, Heidelberg, Germany), rabbit monoclonal anti-ZEB1 (anti-TCF8/ZEB1, 1:1000, clone: D80D3, Cell Signaling), rabbit polyclonal anti-MMP9 (1:1000, catalog number: 3852, Cell Signaling), and rabbit monoclonal anti-CDH1 (1:1000, clone: 24E10, catalog number: 3852, Cell Signaling). Following incubation with the appropriate secondary antibody, the signal was detected with Chemiluminescent Sensitive Plus HRP (BioFx Laboratories,

MD, United States), and images were acquired with the ChemidocTM XRS+ (Bio-Rad Laboratories). For housekeeping protein, mouse monoclonal anti-β-actin (1:2000, clone AC-15, catalog number A1978, Sigma Aldrich) was used. Each experiment was repeated at least twice.

3.4 Gene expression analysis

3.4.1 RNA extraction and retro-transcription

Total RNA was extracted from cells using Trizol® Reagent (Life Technologies, Monza, Italy) following the manufacturer's instructions. RNA concentration was evaluated by measuring the absorbance (optical density, OD) at 260 nm; protein and ethanol contamination were evaluated dividing the absorbance at 260 nm for the absorbance at 280 nm (OD 260/280) or 230 nm (OD 260/230), respectively. All measurements were performed using NanoDrop spectrophotometer (Thermo Scientific).

One μg of total RNA was reverse transcribed using GoScriptTM Reverse Transcriptase Kit (Promega, Milan, Italy). Briefly, RNA and Oligo(dT)15 primers were heated at 70°C for 5 minutes followed by a step on ice for 5 minutes, then the reverse transcription mix added to the primers/RNA mix in a final volume of 20 μl. The reverse transcription mix was composed of 4.0 μl of GoScript™ reaction buffer, 4.0 μl of $MgCl_2$ 25 mM, 1.0 μl of nucleotide mix 10mM, 0.5 μl of Recombinant RNasin® Ribonuclease Inhibitor (40 U/ μl), 1.0 μl of GoScript™ Reverse Transcriptase and 4.5 μl of nuclease free water. After annealing at 25°C for 5 minutes, the extension reaction was performed at 42°C for 60 minutes and reverse transcriptase was then inactivated at 70°C for 15 minutes. The obtained cDNA was diluited 1:10 with MilliQ water and stored at -20°C until use.

3.4.2 qRT-PCR: Gene Expression Assay

qRT-PCR was performed using TaqMan Gene Expression Assays for *HES1* (Hs00172878_m1), *ATOH1* (Hs0094192_s1), *GAPDH* (Hs99999905_m1) or Sybr select Master mix for *JAG1*, *NRARP*,

ZEB1, *MMP9* and *CDH1* (Life Technologies). Primer sequences for Sybr green assays are reported in Table 1. qRT-PCR was performed on iCycler (Bio-Rad Laboratories)

The thermal profile for Sybr select Master mix reactions was: 50°C for 2minutes, 95°C for 2minutes, (95° for 15seconds, 53°C for 15seconds, 72°C for 30seconds) x 40 cycles, 45°C for 10seconds. The thermal profile for TaqMan Gene Expression reactions was: 95°C for 10minutes, (95°C for 15seconds, 60°C for 15seconds) x 40 cycles, 4°C-hold.

Fold induction levels for each gene were analysed by means of the $2^{-\Delta\Delta Ct}$ method, and GAPDH was used as endogenous control. At least two replicates were analysed for each sample.

Gene	Accession n.	Forward Primers (5'-3')	Reverse Primers (5'-3')
Jagged1	NM_000214	AAGGCTTCACGGGAACATAC	AGCCGTCACTACAGATGCAC
NRARP	NM_001004354	GGGCTGCATAGAAAATTGGA	CCCTTTTTAGCCTCCCAGAG
ZEB1	XM_006717499.1	TACAGAACCCAACTTGATCGTCACA	GATTACACCCAGACTGCGTCACA
MMP9	NM_004994.2	TTGACAGCGACAAGAAGTGG	GCCATTCACGTCGTCCTTAT
CDH1	NM_004360.3	GCCGCTGGCGTCTGTAGGAA	TGACCACCGCTCACCTCCGA

Table 1: Primer Sequence for qRT-PCR

3.5 Gene silencing

3.5.1 Notch1 stable silencing

Short hairpin oligonucleotides (shOligos) complementary to shRNA sequences were inserted into the pSuper.puro expression vector according to the manufacturer's instructions (OligoEngine, Seattle, WA), (117). ShOligos targeting different Notch1 exons were as follows: Notch1 (N1S), 5′-ggccgtcatctccgacttca-3′; and Notch1 (N1S1), 5′-gcctcttcgacggctttga-3′. Retroviruses were produced by transient transfection of pSuper.puro retrovectors into Phoenix A packaging cells (kindly provided by Dr Catia Giovannini).

Stable, retroviral transduced populations of cells HT29 NOTCH1$^{-/-}$ were selected in RPMI supplemented with 2µg/ml of puromycin, as previously established by the killing curve.

3.5.2 Metalloproteinase-9 (MMP9) transient silencing

HT29 cells were transfected for 48h with 50nM of a mixture of 4 small interfering RNA (siRNA) against MMP9 (ON-TARGETplus SMARTpool siRNA sequences,Dharmacon, Thermo Fisher Scientific, Cultek SL, Madrid, Spain), using Dharmafect transfection reagent-1 (Thermo Fisher Scientific, T-2001-01). A non-targeting siRNA (D-001810-10-05, Dharmacon) was used as a negative control (scramble).

3.6 Cell viability assay

Cell sensitivity to EPA-FFA was evaluated by the 3-(4,5-dimethylthiazol-2-yl)-2, 5-diphenyltetrazolium bromide assay (MTT, Sigma Aldrich) assay. This colorimetric assay is a reliable way to examine cell viability since this latter is directly proportional to the metabolic activity of the mitochondria. Indeed, MTT is a water-soluble tetrazolium salt metabolized only by living cells and converted into formazan by the action of a dehydrogenase enzyme. The formazan is violet and appears as insoluble material at the bottom of the culture plate. The formazan is solubilized in DMSO to form a purple solution whose intensity is proportional to cell density.

HT29 and HCT116 cells were seeded in 96-well plates at a density of 5 and 3x10^3 cells, respectively, and incubated for 72 h prior to treatment with EPA-FFA (0-200µM). Following treatment, the medium was removed and the cells were washed with PBS.Then, MTT (5 mg/mL) was added and the cells were incubated at 37°C for 4h. After the incubation, the medium was discarded and 100uL of solubilization reagent (10% SDS in HCl 0.01N) was added in each well. Then, the formazan formed was dissolved in DMSO (200µl) andthe day after, the absorbance at 560 nm was measured in a microplate reader (GloMaxÂ®-Multi Microplate Reader (Promega

Corporation, Madison, WI, USA) The absorbance values were expressed as percentage of control (untreated cells). Each experiment was performed in quintuplicate.

3.7 Mucosal fatty acid analysis

In order to examine the relative content of EPA into the cellular membranes of control and treated cells, the whole amount of lipids was extracted from the cells, chemically treated -as reported below- and the content was analyzed by Gas Cromatography-Mass Spectrometry (GC-MS).

3.7.1 Lipid extraction

The cellular pellets were resuspended in ice-cold PBS and transferred with Pasteur pipettes in Sovirel extraction tubes, washed with 3 ml of chloroform-methanol mixture ($CHCl_3$/MetOH 1:2 vol/vol) in presence of the antioxidant butylated hydroxytoluene (BHT 0.01%) and shaked for 30 minutes at room temperature.Then, samples were centrifuged for 10 minutes at 2000 x G at room temperature and the upper solvent layer was transferred in a new Sovirel tube. The extraction was repeated with 2 ml of solvent and the supernatant layer combined. The solvent fraction was then re-extracted with 3 ml of $CHCl_3$/H_2O (1:1 - BHT 0.01%), vortexed and spinned, (2000 x G, 5 min, 25°C); the inferior solvent phase was transferred to a new Sovirel tube and frozen at –20°C untilthe transesterification.

3.7.2 Transesterification

The solvent phase was evaporated under a stream of nitrogen and 2 ml of KOH/MetOH solution (0.5M + 0.01% BHT) were added, the tubes carefully closed and heated at +80°C for 10 minutes in a dry thermal block. When the temperature of the solution reached 25°C 1 ml of BF3: MetOH solution was added to each sample and the tubes were warmed at +80°C in the thermal block for 10 minutes to develop a methyl ester mix.

3.7.3 Extraction of methyl esters

Methyl esters were extracted adding 3 ml of hexane to each sample. The samples were then vortexed for 30 seconds and spinned at 2000xG for 10 minutes at room temperature. The

supernatant solvent phase was carefully recovered and transferred to a new glass tube. This extraction process was repeated with 2 ml of hexane. Then, the hexane was evaporated under a stream of nitrogen to reduce the volume to 1 ml which was then transferred to a glass auto sampler vial. The tube was washed with 500 µl of hexane and the sample evaporated to dryness, redissolved with 20 µl of ciclohexane for the analysis and frozen at –20°C until injected.

3.7.4 Gas Cromatography-Mass Spectrometry (GC-MS) conditions

GC-MS analysis was carried out using an Agilent HP6890 GC with PTV Injector and MS with aHP5973 mass detector; The column is SUPELCO SPTM-2330 (30mt x 0.25 mm x 0.2 µm film thickness) column. Carrier gas is Helium at 0.5 ml/minutes, in constant pressure mode; Injection cycle is in Solvent Vent mode, starting from 60° and ramps to 220°C; column temperature was from 100°C for 1.25 minutes, then was programmed to rise to 185°C at 30 °C and to 205°C at 5 °C/minutes; total GC run time was 32 minutes 1-4 µl samples was injected to GC-MS analysis. MS operates in EI mode, at 70 eV; Quadrupole temperature is 150°C; Ion source and GC interface were respectively 230°C, 280°C; Full data scan from m/z 40 to m/z 550.

3.7.5 Data processing and quantification

Retention times and peak area of analytes were determined by the Enhanced Data Analysis integration system of G1701 DA Agilent software. The percentage of analytes was calculated from the sum of the peak area of all analytes of interest using the following equation:

$$\text{Analyte percentage} = \frac{\text{Analyte Peak area} * 100}{(\Sigma \text{ areas of all identified peaks})}$$

3.8 Invasion assay

The invasive potential of HT29 and HCT116 cells was assessed by chemoinvasion assay (118). Briefly, poly-vinylpyrrolidone-free polycarbonate filters (Millipore, Co. Cork, Ireland) with 8 μm pores were coated with Matrigel (Sigma-Aldrich) and positioned in the middle part of the Boyden blind-well chambers (New Technologies Group, Monza e Brianza, Italy). Fresh RPMI supplemented with 20% FBS was placed in the lower part of the chamber as chemoattractant. After CM and/or EPA-FFA treatment, 7×10^4 HT29 and HCT116 cells were resuspended in serum-free medium and added to the upper part of the chambers. The chambers were then incubated at 37°C in humidified 5% CO_2. At the end of incubation, non invading cells were removed from the upper surface of the filters with cotton swabs. Invading cells in the lower surface were then fixed for 1 minutes in ethanol 95% and stained for 10 min with 0.5% w/v with Giemsa (Sigma Aldrich). Photographs were taken with an Olympus CKX41 inverted microscope (Olympus Italia, Milan, Italy), equipped with an Olympus C5060-ADU camera (Olympus Italia). For each sample, ten random optical fields at ×200 of total magnification were analyzed and the mean number of invading cells was counted.

3.9 Gelatin Zymography

MMP9 activity was determined by gelatin zymography as previously described (119) with minor modifications. Cells were treated with CM for 12h, then CM was removed and cells were incubated o.n. in serum-free medium. The media was collected, centrifuged (400g, 5minutes at 4°C) to remove cells and debris, and precipitated using three volumes of Methanol at -20°C o.n. Proteins were precipitated with 1:4 (vol/vol) ice-cold methanol o.n. Proteins were pelleted by centrifugation at 6500G at 4°C for 40 minutes and the pellets were resuspended in PBS. Protein concentration was determined using Lowry's assay. After solubilization with sample buffer (not containing reducing agents, but only SDS at 8% to charge proteins-Tris HCl pH6.8, SDS 8%, Glycerol 40%, Bromophenol blue 0,4%), 20 μg of proteins were loaded in 10% polyacrylamide gels, previously

co-polymerized with 1% gelatin. After electrophoresis, the gels were washed twice in 2.5% in H_20 Triton X-100 and incubated o.n. in an activation buffer (50 mM Tris–HCl supplemented with 5 mM $CaCl_2$). The digested bands on the gels were highlighted with Comassie brilliant blue R-250 staining and de-stained with 50% methanol and 10% acetic acid in distilled water. MMP9 proteolytic activity was quantified using ChemiDocTM XRS+(Biorad, CA, USA).

3.10 Statistical analysis

Data were analyzed with Graphpad 5.0 Software (GraphPad Software Inc., CA, USA). Whenever necessary, the values were transformed using the function Y=log(Y) to stabilize the variances. The means of two unmatched groups were compared using the unpaired T test, while the one-way ANOVA followed by Tukey's or Dunnet's post hoc tests were used to compare the means of three or more groups. The data are shown as Mean±SEM. P values less than 0.05 were regarded as statistically significant.

4. RESULTS

4.1 Conditioned Medium production

First, we differentiated the THP1-monocytes into macrophages using PMA and we stimulated them with LPS; then, we collected the cytokine-enriched supernatant. Through this approach we obtained a complex and heterogeneous *stimulus* able to mimic of the pro-inflammatory microenvironment.

4.1.1 Differentiation of THP1 from monocyte to macrophages

It is known that monocytes are highly plastic and heterogeneous, and that they are able to change their functional phenotype. Evidences from murine and human studies have suggested that they can differentiate into tissue macrophages in response to environmental stimulation. Also, based on specific markers of cellular surface, it is possible to identify the specific subset of differentiated-cells (120).

FACS analysis of PMA-differentiated THP1 cells showed increased expression of specific markers of macrophages, namely CD11b ($p=0.0027$) and CD14 ($p=0.0507$), compared to untreated THP1, as shown in Figure 13.

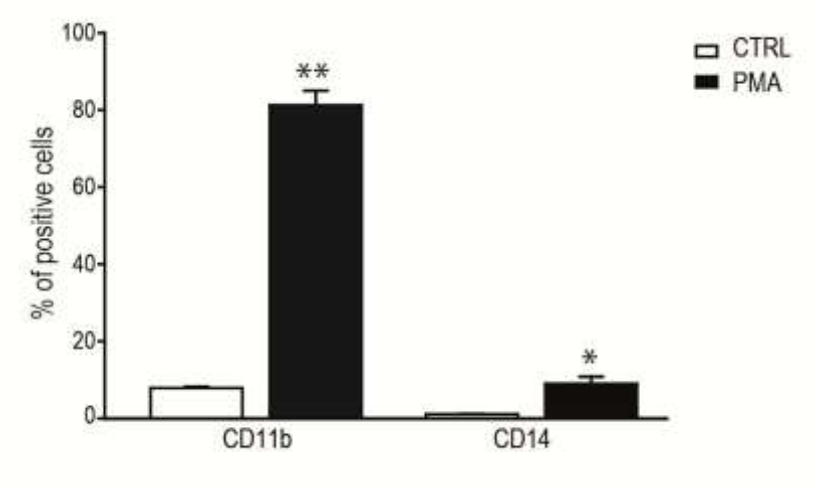

Figure 13: FACS analysis for the expression of CD11b and CD14 in THP1 cells untreated (CTRL) or treated with PMA.

4.1.2 Stimulation of THP1induced the release of pro-inflammatory mediators

Macrophages play a key role in the orchestration and execution of the inflammatory processes. Upon differentiation, the macrophages lose their ability to replicate and their defense functions are markedly enhanced, allowing them to participate in the inflammatory and immune responses (121). In the *in vitro* systems, Lipopolysaccharide (LPS) derived from gram-negative bacteria is considered to be the most potent activator of the macrophage secretory response (122). In our model, the stimulation with LPS leads THP1 to produce a Conditioned Medium (CM) enreached with different pro-inflammatory mediators, as shown in Figure 14.

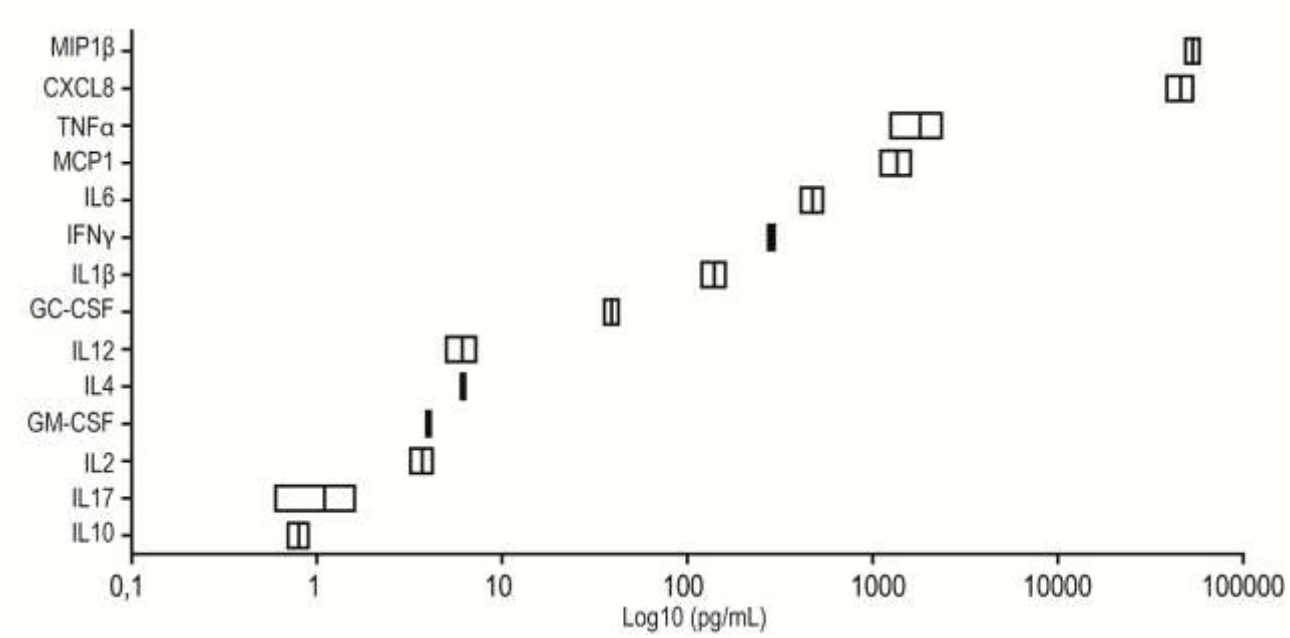

Figure 14: Explorative analysis of inflammatory mediators contained in the Conditioned Medium (CM) from PMA-differentiated THP1 after activation with LPS. Analysis was performed with a multiplex bead-based sandwich immunoassay to detect 14 inflammatory mediators; concentrations (pg/ml) are reported on a log10 scale.

Moreover, among the 6 most expressed pro-inflammatory mediators, we found that IL-6 ($p=0.0263$), CXCL8 ($p=0.004$), TNF-α ($p=0.0053$) and MIP-1β ($p<0.0001$) significantly increased in the supernatant from LPS stimulated-THP1 compared to the unstimulated counterpart, while no differences were found for IFN-γ and MCP-1 (Figure 15).

These results indicate that the CM produced by the PMA-differentiated THP1cells represents a complex pool of mediators, able to resembles a multi-inflammatory *stimulus*.

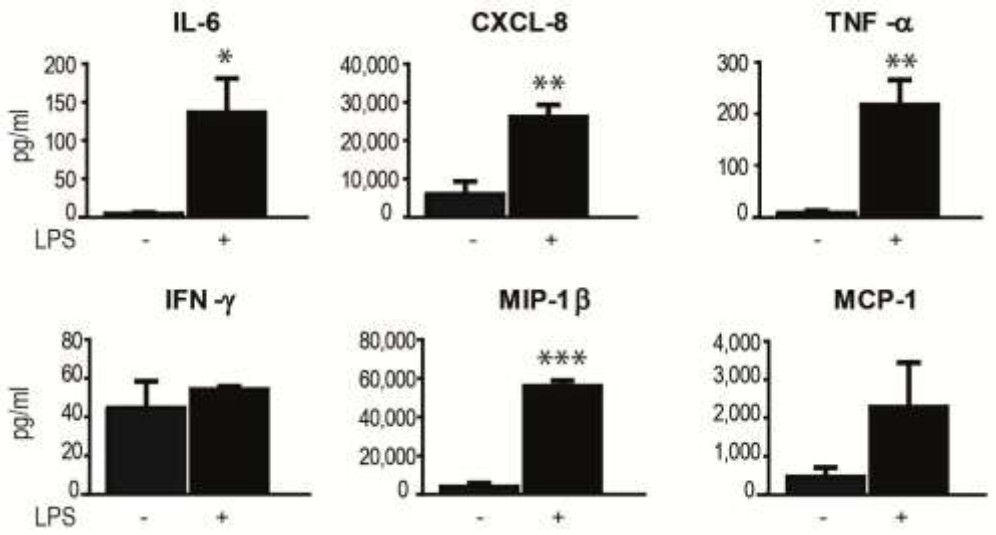

Figure 15: Pro-inflammatory mediators in the conditioned medium (CM) from PMA-differentiated THP1 before and after activation with 50 ng/ml of LPS for 1h. Two replicates were analysed for each sample. Number of replicates (n)=2, number of independent experiments (N)=2. *= $p<0.05$, **=$p<0.01$, ***=$p<0.001$, unpaired t-test.

4.2 The Conditioned Medium promotes Notch1 pathway in CRC cells

To determine whether the pro-inflammatory *stimulus* represented by the THP1-derived CM could drive the activation of Notch1 pathway, we incubated CRC cell lines with the CM and we analysed the effect of incubation both at a tradutional and a transcritpional level.

4.2.1Effect of CM exposure on Notch1 pathway

We found that upon 12 hours of CM exposure, the protein levels of the Notch1 Intracellular Domain (NICD) and the ligand of Notch1 importantly increases JAG1both in HT29 and HCT116 cell lines (Figure 16). Notably, these data indicate that CM induces the activation of Notch1 pathway, since it has been demonstrated that the binding of Jagged1 to the Notch1 receptor leads to the cleavage of Notch1 and to the consequent formation of the Intracellular Domain of Notch1 (NICD) which then traslocated into the nucleus (61).

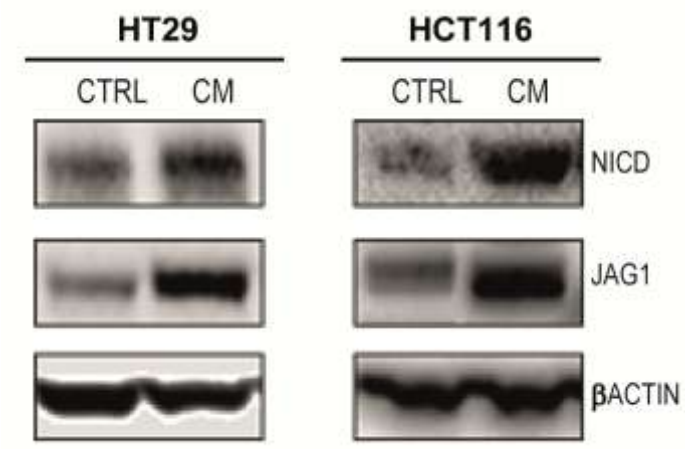

Figure 16: Western Blot analyses for NICD and JAG1 in HT29 and HCT116 exposed to CM for 12h. β-ACTIN was used as housekeeping protein. Each experiment was repeated at least three times.

4.2.2 Effect of CM exposure on transcriptional activity of Notch1

To demonstrate that the up-regulation of the proteins involved in Notch1 pathway had an effective repercussion on the transcriptional activity of Notch1, we performed the *qRT-PCR* for the downstream target genes of Notch1. Particularly interesting was the evaluation of *NRARP*, since it has been demonstrated that it is the most reliable intestinal marker of Notch1 activation (72).

We found that the CM-driven up-regulation of Notch1 pathway in HT29 and HCT116 cells was confirmed at mRNA level by a significant increase of the Notch1 target *NRARP* (p=0.0011 for HT29 and p=0.0023 for HCT116, CTRL vs CM), and a consensual decrease of *ATOH1* (p=0.0027 for HT29 and p=n.s for HCT116, CTRL vs CM) together with the increased expression of the Notch1 ligand *JAG1* (p=0.0443 for HT29 and p=0.0012 HCT116, CTRL vs CM). Interestingly, no changes were observed in the level of the *HES1* transcripts after Notch1 activation (Figure 17).

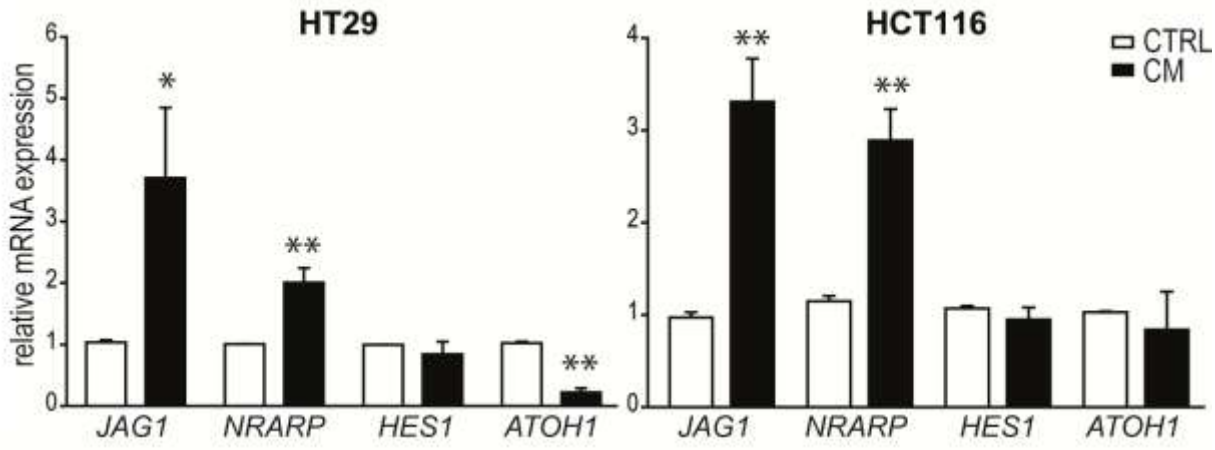

Figure 17: qRT-PCR for *JAG1*, *NRARP*, *HES1* and *ATOH1* in HT29 and HCT116 cells incubated in CM.Statistical significance was calculated on logarithmic transformed values using unpaired t-test, (n=3, N=4). *= p<0.05; **=p<0.01; ***=p<0.001. *GAPDH* was used as housekeeping gene.

4.3 Treatment with single proinflammatory mediators

Since our hypothesis was that a multi-cytokine *stimulus*, rather than the effect of a single inflammatory mediator, induces the activation of Notch1 signaling in our model, we also tested the effect of single IL-6, CXCL8 or TNF-α exposures, given their abundance in the CM on HT29 cells. Then, we analysed NICD and JAG1 protein level. Effectively, our data show that the treatment with single cytokines did not increase the protein level of NICD and JAG1 (Figure 18).

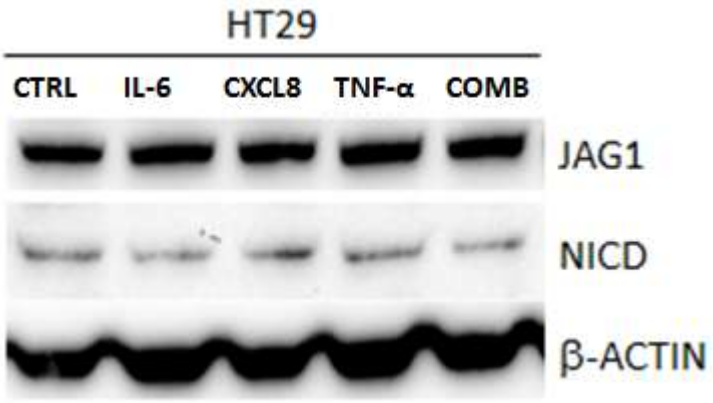

Figure 18: Western Blot analyses for NICD and Jagged1 in HT29 treated with single cytokines. IL-6 (100 ng/ml) CXCL-8 (1µg/ml) or TNF-α (100 ng/ml) were used alone or in combination (COMB). βactin was used as housekeeping protein.

4.4 The Conditioned Medium promotes EMT in CRC cells

To date, it has been demonstrated that many cytokines are known to promote EMT in cancer cells (93), (123), (124), (125). Therefore, we decided to check EMT modulation in our model. In particular, we focused on ZEB1 and its direct target e-cadherin (CDH1), which play a central role in EMT, and on MMP9, since a modulation of NICD in MMP9-overexpressing cells has been recently demonstrated (80).

4.4.1Effect of CM exposure on proteins of EMT

We found that the protein levels of ZEB1 and MMP9 were increased in both HT29 and HCT116 treated with CM compared to the controls and, concomitantly, we found a modest reduction of E-Cadherin (CDH1) upon CM exposure in HCT116 (Figure 19).

4.4.2 Effect of CM exposure on transcriptional factors involved in EMT

The results reported above were confirmed by a significant increase of *ZEB1* ($p=0.008$ for HT29 and $p=0.0373$for HCT116, CTRL vs CM) and *MMP9* ($p=0.0224$ for HT29 and $p<0.0001$ for HCT116, CTRL vs CM) transcripts and by a consensual but not significant decrease of *CDH1* in CM-treated cells compared to the controls (Figure 20).

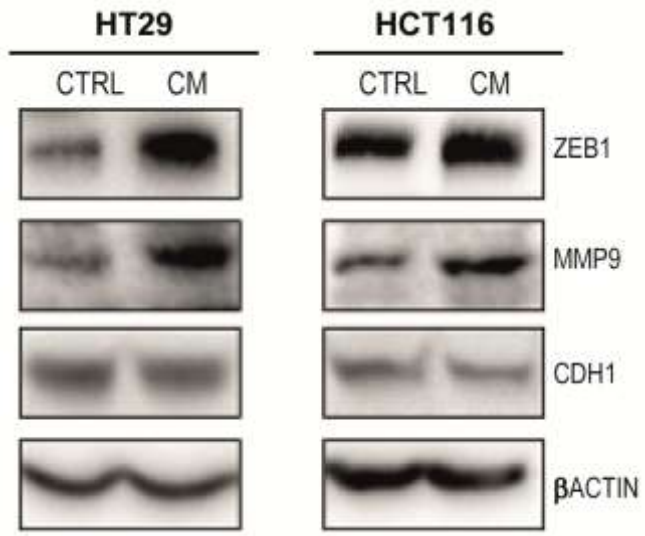

Figure 19: Western Blot analyses for ZEB1, MMP9, and CDH1 in HT29 and HCT116 exposed to CM. β-ACTIN was used as housekeeping protein. Each experiment was repeated at least three times.

Taken together, these results suggest that the inflammatory microenvironment, represented by our cytokine-enreached-CM, can contextually activate Notch1 signaling and EMT both in HT29 and in HCT116 cells.

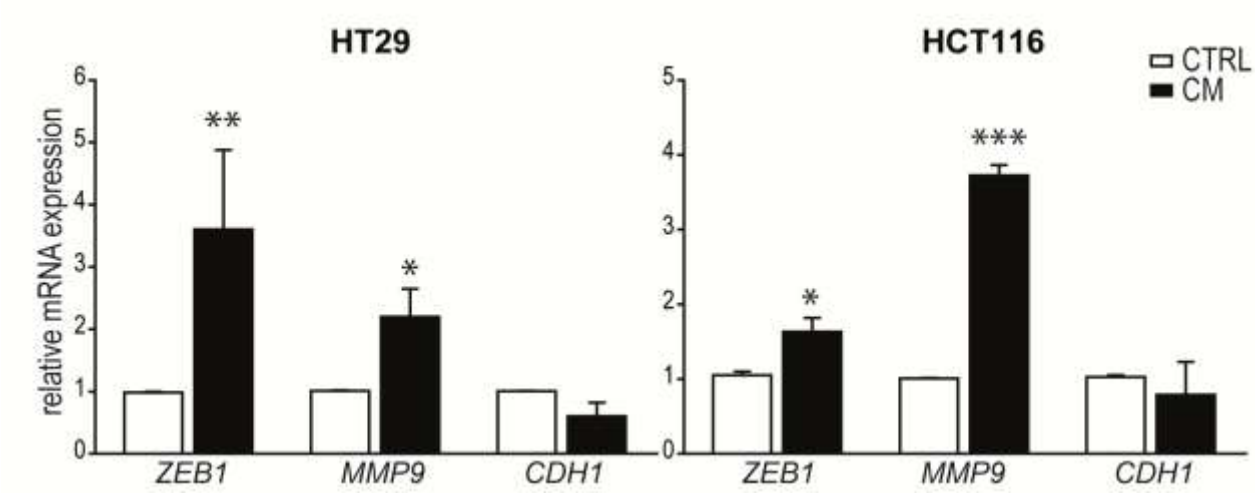

Figure 20: qRT-PCR for *ZEB1, MMP9* and *CDH1* in HT29 and HCT116 cells incubated in CM. *GAPDH* was used as housekeeping gene. Statistical significance was calculated on logarithmic transformed values using unpaired t-test, (n=3, N=4 for HT29 and n=3, N=3 for HCT116). *= $p<0.05$; **=$p<0.01$; ***=$p<0.001$

4.5 Notch1 up-regulation depends on MMP9 expression upon inflammation

To better clarify the link between pro-inflammatory microenvironment, Notch1 signaling and EMT modulation, we tested the effect of CM both in Notch1- or MMP9-silenced HT29 cells.

4.5.1 The effect of Notch1 silencing

Intriguingly, our data show that the MMP9 induction upon CM exposure persisted even after Notch1 silencing. Accordingly, when we evaluated the mRNA expression of EMT mediators in CM-treated HT29 Notch1$^{-/-}$ cells, we still found a significant up-regulation of *ZEB1* and *MMP9* ($p=0.0371$ and $p=0.0336$, respectively) in Notch1$^{-/-}$ CM vs Notch1$^{-/-}$ CTRL (Figure 21), suggesting that the CM-driven induction of the EMT mediators was independent or precedes the Notch1 activation.

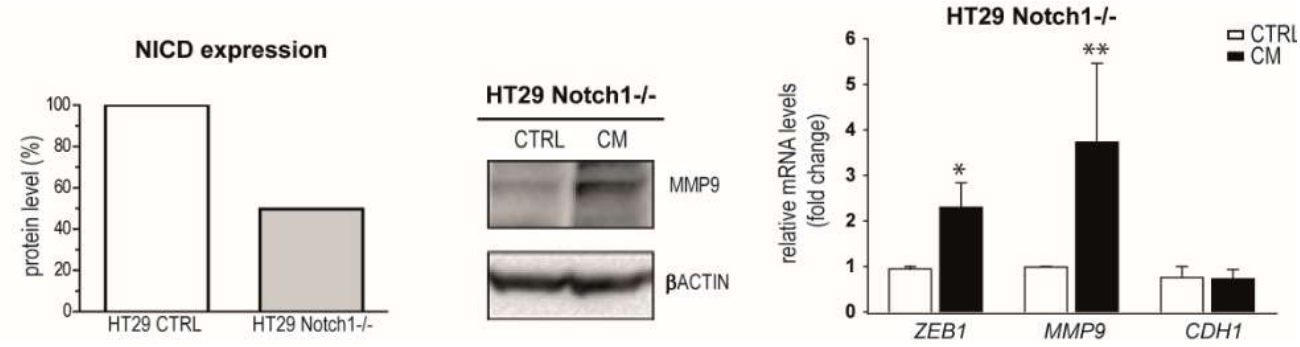

Figure 21: Notch1 silenced cells under inflammatory conditions. (A) NICD protein level in HT29 (CTRL) and NOTCH1 stably-silenced HT29 (NOTCH1$^{-/-}$). (B) Western Blot analyses for MMP9 in NOTCH1-silenced HT29 cells exposed to CM. Each experiment was repeated three times. (C) qRT-PCR for *ZEB1, MMP9* and *CDH1* in NOTCH1 silenced-HT29 cells incubated in CM. Statistical significance was calculated on logarithmic transformed values using unpaired t-test, (n=3, N=3). *= p<0.05; **=p<0.01; ***=p<0.001.

4.5.2 The effect of MMP9 silencing

To eventually demonstrate that MMP9 causes the activation of Notch1, we performed the silencing of MMP9, expecting that under this condition the CM-driven NICD overexpression did not occur. Therefore, we transiently silenced MMP9 in HT29 cells. Importantly, we found that the protein level of NICD did not increase upon CM compared to its scramble control. Moreover, in MMP9-silenced cells the transcriptional level of JAG1 and NRARP were not increased by CM stimulation (Figure 22).

Taken together, our data show that inflammation up-regulates MMP9 which is in turn responsible for the activation of Notch1 pathway in CRC cells.

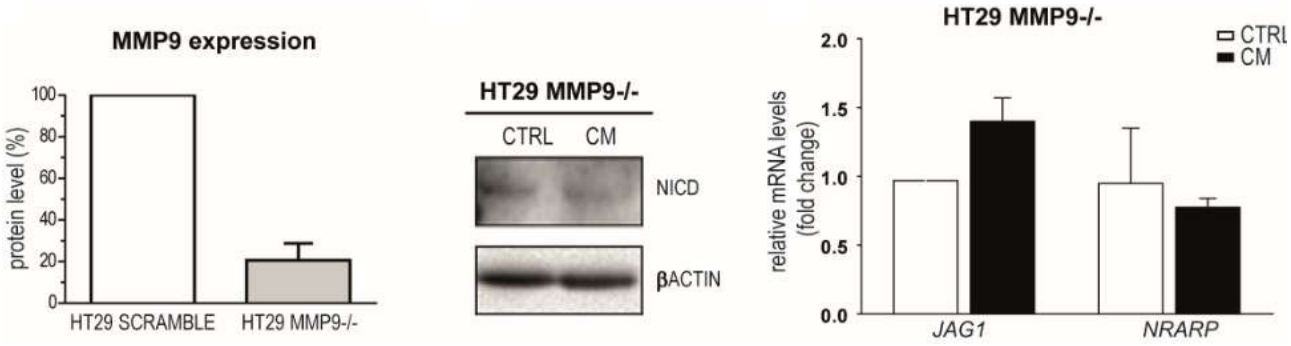

Figure 22: MMP9-silenced HT29 cells under inflammatory conditions MMP9 protein level in scramble and MMP9 transiently silenced-HT29 ($MMP9^{-/-}$). (E) Western Blot analysis for NICD in MMP9-silenced HT29 cells exposed to CM for 12h. Each experiment was repeated twice. (F) qRT-PCR for *JAG1* and *NRARP* in MMP9-silenced HT29 and HCT116 cells incubated in CM, Statistical significance was calculated on logarithmic transformed values using unpaired t-test, (n=3, N=2). *= $p<0.05$; **=$p<0.01$; ***=$p<0.001$. GAPDH was used as housekeeping gene.

4.6 EPA-FFA treatment counteracts inflammatory-driven Notch1 activation

Aiming at unravel new possible molecular mechanisms to explain the protective role of EPA in CRC, in this study EPA-FFA (ALFA, SLA Pharma Switzerland) was used for investigating its effect on CM-driven Notch1 and EMT activation.

4.6.1 The establishment of EPA-FFA pre-treatment

Firstly, HT29 and HCT116 were pre-treated for 72h with different dose of EPA-FFA in order to establish the range of toxicity of the substance. We found that EPA-FFA was non-cytotoxic up to 150 μM, as established by MTT assay (Figure 23). For this reason, we decided to treat the cell lines with 50μM of final concentration, which was a very lower dose respect to the limit of toxicity.

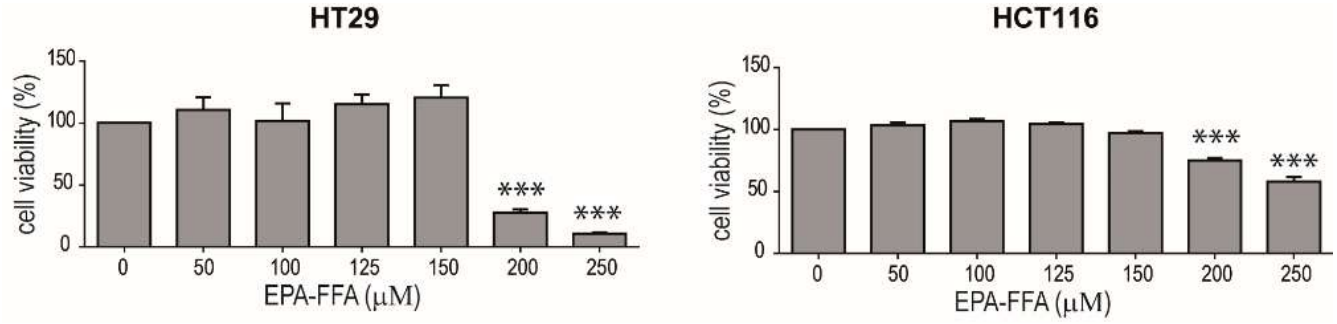

Figure 23: Cell viability of HT29 (left panel) and HCT116 (right panel) treated with EPA-FFA. Each experiment was performed in quintuplicate. Concentrations of EPA-FFA lower than 200 μM (HT29) and 150 μM (HCT116) did not cause cytotoxicity (ANOVA $p<0.0001$, Dunnet's test).

Then, we tested the incorporation level of EPA into the cellular membrane, in order to demonstrate that EPA-FFA was effectively absorbed by the cells. We found that this treatment led to a 36% and 19% of EPA incorporation into HT29 and HCT116 cellular membranes, respectively (Figure 24). We also optimized a prolonged treatment on HT29 (14 days of EPA-FFA) and observed that the levels of EPA incorporation were similar after 72h or 14 days of EPA-FFA (Table 2). Therefore, we decided to incubate our cells with EPA-FFA for 72h.

Figure 24: Relative abundance of EPA into the cellular membranes. Abundances for HT29 (left panel) and HCT116 (right panel) treated or not with 50 uM of EPA-FFA for 72h.

TREATMENT	Palmitic	Stearic	Oleic	Linoleic	Linolenic	ARA	EPA	DPA	DHA
CTRL 72h	22,3	23,0	41,5	7,6	0,4	2,56	0,64	0,8	1,06
CTRL 72h	22,3	23,0	41,5	7,6	0,4	2,56	0,64	0,8	1,06
EPA-FFA 72h	13,4	23,7	16,7	4,1	0,7	1,26	36,32	3,2	0,63
EPA-FFA 72h	13,4	23,6	16,9	4,1	0,9	1,34	36,20	3,0	0,55
CTRL 14days	22,9	22,2	43,2	4,9	0,5	2,91	0,99	1,1	1,28
CTRL14days	16,3	19,4	52,2	5,5	0,4	3,27	0,92	0,8	1,16
CTRL 14days	20,4	23,8	44,6	4,7	0,5	2,89	0,86	0,8	1,33
EPA-FFA 14days	19,0	28,0	19,4	2,2	1,1	1,40	25,16	2,7	1,02
EPA-FFA 14days	18,4	28,5	19,9	2,4	0,6	1,38	25,13	2,6	1,01
EPA-FFA 14days	19,8	28,2	18,5	2,2	1,1	1,57	25,33	2,3	0,98

Table 2: Relative abundances of Fatty acids after a 72h or 14 days treatment with EPA-FFA.

4.6.2 Effect of EPA-FFA treatment on CM-induced Notch1 pathway

After 72h of EPA-FFA pre-treatment, HT29 and HCT116 were incubated with CM for 12h and Notch1 pathway was further analysed.

In accordance to our hypothesis, EPA-FFA was able to reduce the CM-driven induction of JAG1 and NICD both in HT29 and HCT116 cells (Figure 25 A and B). Accordingly, the EPA-FFA pre-treatment alone did not significantly change the mRNA levels of *JAG1*, *NRARP*, *HES1* and *ATOH1* (p=n.s. CTRL vs EPA) but was able to significantly counteract their increase in both HT29 and HCT116 CM-treated cells ($p<0.01$ and $p<0.05$ CTRL vs CM; p=n.s. CTRL vs EPA+CM, HT29 and HCT116 respectively), (Figure 25 C and D). However, pre-treatment with EPA-FFA did not reverse the profound *ATOH1* down-regulation in HT29 cells ($p<0.001$ CTRL vs EPA+CM) obtained after CM incubation.

Taken together, our data demonstrate that pre-treatment with a non-cytotoxic dose of EPA-FFA was able to counteract the activation of Notch1 signaling obtained upon the incubation with the mixture of pro-inflammatory mediators represented by CM.

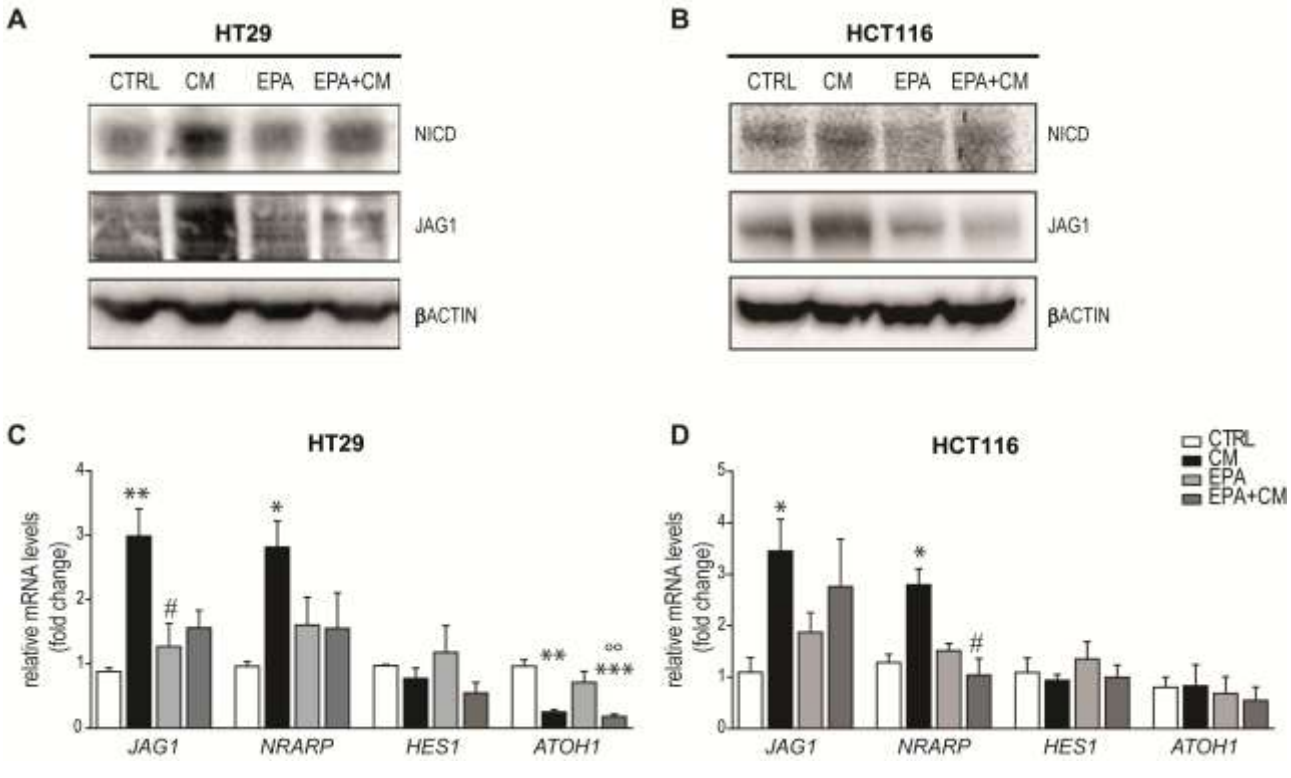

Figure 25: EPA-FFA represses inflammatory-driven NOTCH1 activation. Western Blot analyses for NICD and JAG1 in HT29 (A) and HCT116 (B) in incubated with CM (12h) and/or pre-treated with EPA-FFA (72h). β-ACTIN was used as housekeeping protein. (C) qRT-PCR for *JAG1* (ANOVA, p=0.0085), *NRARP* (ANOVA, p=0.0440), *HES1* (ANOVA, p=n.s.) and *ATOH1* (ANOVA, p=0.0006) in HT29 (left panel) treated with EPA-FFA (72h) and/or CM (12h). (D) qRT-PCR for *JAG1* (p=0.0509), *NRARP* (p=0.0136), *HES1* (p=n.s.) and *ATOH1* (p=n.s.) in HCT116 (right panel) treated with EPA-FFA (72h) and/or CM (12h). Data were corrected by logarithmic transformation and analyzed by One-way ANOVA and Tukey's Test for multiple pairwise comparisons (n=3, N=3). *= p<0.05, **=p<0.01, ***=p<0.001 compared to CTRL; #= p<0.05, ##=p<0.01, ###=p<0.001 compared to CM; °= p<0.05, °°=p<0.01, °°°=p<0.001 compared to EPA-FFA.

4.7 Effect of EPA-FFA on CM-driven MMP9 activation

To better clarify the role of EPA-FFA in our model, focusing in particular on the ability of EPA-FFA to prevent the EMT phenotype induced through the incubation with CM, we assayed MMP9 activity by gelatin zymography on CRC cells treated with CM alone, treated with EPA-FFA alone or treated with CM after a 72h EPA-FFA pre-treatment.

The gelatin zymography revealed that CM was able to induce an increase of MMP9 activity both in HT29 and HCT116 ($p<0.05$ and p=n.s. CTRL vs CM, respectively). Importantly, treatment with EPA-FFA alone did not induced changes in term of MMP9 activity, but we found that pre-treatment with EPA-FFA reduces the CM-induced MMP9 activity in HCT116 (p=n.s. CM vs EPA+CM), although not reaching a statistical significance.

Interestingly, we also found a decreasing trend of mRNA levels for *ZEB1* (p=n.s. in HCT116 and HT29) and *MMP9* ($p<0.05$ in HCT116, CTRL vs CM; p=n.s. CTRL vs EPA+CM; p=n.s. in HT29) in samples pre-treated with EPA-FFA and incubated with CM compared to samples only incubated with CM, while EPA-FFA alone did not induced variations in the expression of tested mRNA (Figure 26B).

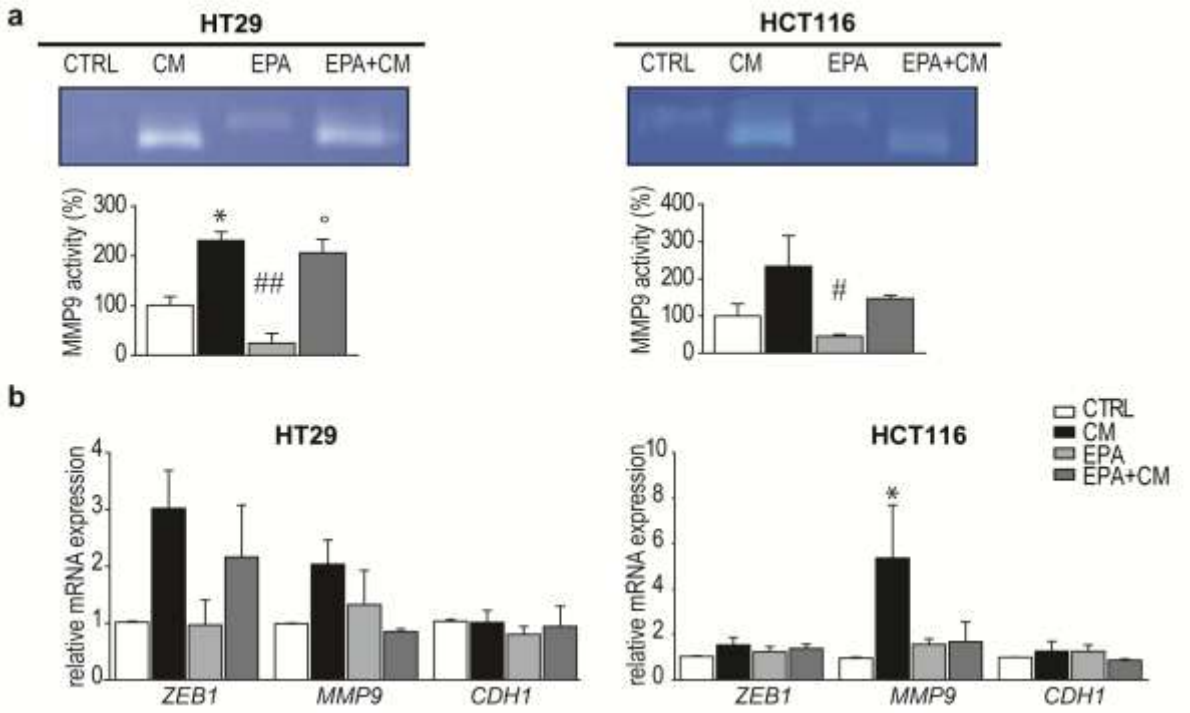

Figure 26: Effect of EPA-FFA on CM-induced MMP9 activation and invasion. (A) Gelatin zymography in response to EPA-FFA (72h) and/or CM (12h) treatment in HT29 (left panel) and HCT116 (right panel). Bars indicate Mean±SEM of densitometric values of MMP9 form normalized to the corresponding CTRL values (ANOVA p=0.0067 for HT29 and p=0.0473 for HCT116, (N=2). (B) qRT-PCR for ZEB1 (ANOVA p=n.s for HT29 and HCT116), MMP9 (ANOVA p=n.s for HT29 and p=0.0525 for HCT116) and CDH1 (ANOVA, p=n.s for HT29 and HCT116) in HT29 and HCT116 EPA-FFA and/or CM treated cells (n=2; N=3). Analyses were performed on logarithmic transformed data. After the ANOVA global test, Tukey's post hoc test was used for multiple pairwise comparisons. *= $p<0.05$, **=$p<0.01$, ***=$p<0.001$ compared to CTRL; #= $p<0.05$, ##=$p<0.01$, ###=$p<0.001$ compared to CM; °= $p<0.05$, °°=$p<0.01$, °°°=$p<0.001$ compared to EPA-FFA.

4.8 EPA-FFA treatment counteracts cell invasion

Finally, we decided to analyse the phenotypical effect of CM and EPA-FFA treatment on CRC cells. We opted for the evaluation of the invasive behaviour, since it is known that EMT led to an augmented capability to invade and that this latter is one of the dominant program in human colon cancer (97).

We achieved that CM significantly induced invasiveness in both HT29 and HCT116 ($p<0.05$ for both compared to controls) and pre-treatment with EPA-FFA strongly reduced this effect (p=n.s. for both compared to controls), as shown in Figure 27.

In conclusion, these data indicate that in our *in vitro* model a non-cytotoxic treatment with EPA-FFA is able to reduce the Epithelial to Mesenchymal Transition and to prevent invasiveness driven by inflammatory conditions.

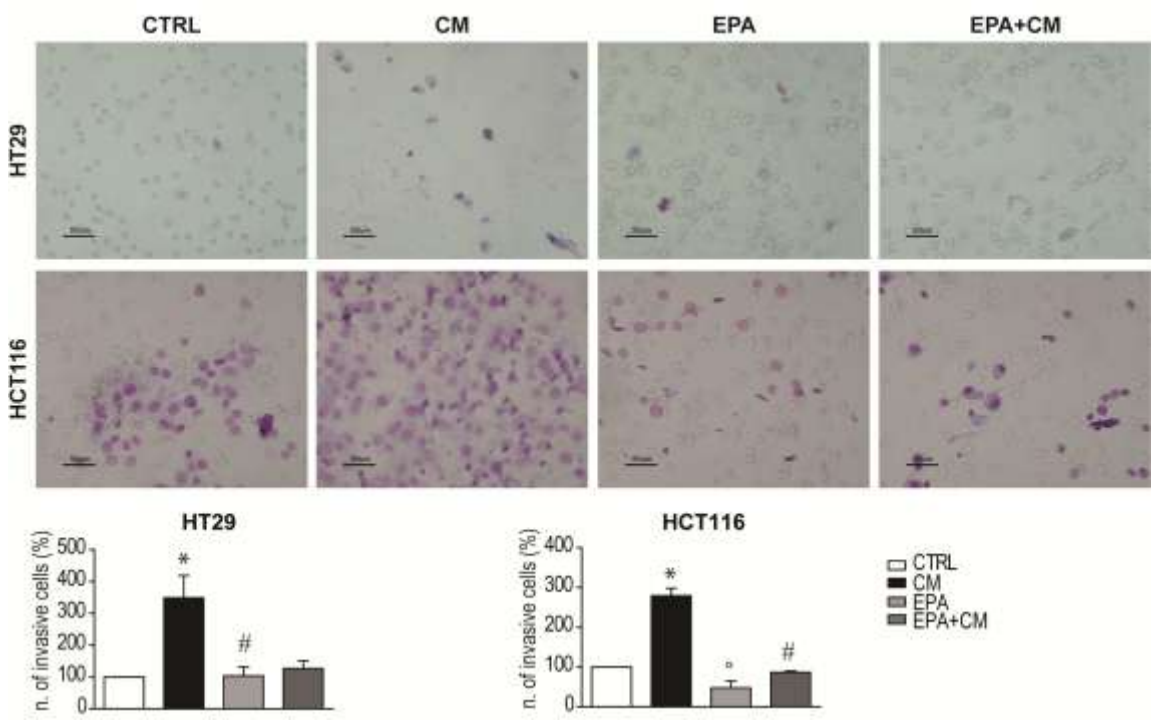

Figure 27: Matrigel invasion assay of HT29 and HCT116 treated with EPA-FFA and/or CM. Bars indicate Mean±SEM of number of invasive cells/chamber normalized to the corresponding CTRL values (ANOVA p=0.0284 for HT29 and p=0.0007 for HCT116), (n=5, N=2). Analyses were performed on logarithmic transformed data. After the ANOVA global test, Tukey's post hoc test was used for multiple pairwise comparisons. *= $p<0.05$, **=$p<0.01$, ***=$p<0.001$ compared to CTRL; #= $p<0.05$, ##=$p<0.01$, ###=$p<0.001$ compared to CM; °= $p<0.05$, °°=$p<0.01$, °°°=$p<0.001$ compared to EPA-FFA.

5. DISCUSSION

The aim of this study was to investigate the role of a complex inflammatory *stimulus*, represented by the mix of mediators obtained in the Conditioned Medium (CM) from stimulated macrophages, on the modulation of Notch1 pathway. The data presented here show that the exposure of CRC cells to CM strongly up-regulates Notch1 signaling, inducing changes in Epithelial to Mesenchymal Transition (EMT) markers and enhancing cell invasion; we also found that Notch1 pathway depends on MMP9 expression under inflammatory conditions. Moreover, this work aimed at studying the possible protective role of Eicosapentaenoic Acid in the free fatty acid form (EPA-FFA) on the above-mentioned molecular mechanism. We demonstrate, for the first time, that the treatment with EPA-FFA, used at a non-cytotoxic concentration, is able to counteract the effect of inflammation both on Notch1 cascade and on cell invasion.

A growing interest in the role of the inflammatory microenvironment in tumorigenesis has been recently emerged, and, with the purpose of studying the related molecular mechanisms, the use of a Conditioned Medium has already been employed (CM), (126). This approach points at analysing the combined effect of different inflammatory mediators, instead of the role of single molecules, thus representing a model more similar to the *in vivo* scenarios. Notably, it has been already reported that the inflammatory mediators expressed in our CM are crucially involved both in CAC and sporadic CRC (47). Interestingly, when we applied each single pro-inflammatory factor (IL-6, CXCL8 and TNFα) to HT29 and HCT116, we did not obtain the same level of Notch1 induction found after the incubation with CM, even if these cytokines were chosen because of their major abundance in CM. We observed a similar result also combining IL-6, CXCL8 and TNFα, indicating that the *stimulus* represented by CM is so complex that cannot be reproduced only by four mediators. Similarly to the present work, in which is shown that CM up-regulates the Notch1 pathway in CRC cells, Lin and colleagues found a marked increase of Notch1 by incubating CRC cells in a Conditioned Medium collected from cultured mesenchymal stem cells. However, albeit

they reported an increase of full length Notch1 expression due to IL-6 treatment, in our study the level of the active domain of Notch1 protein was not affected by this cytokine (82). In our model, the induction of Notch1 pathway is confirmed by the concordant modulation of its downstream targets *NRARP* and *ATOH1*, while no changes were observed for HES1, in agreement with the finding that it can be also controlled by Notch1-independent signaling pathways (127). Many other reports indicate a pro-tumorigenic role of Notch1 in relation to inflammation in models of CRC. For instance, it has been reported that the crosstalk between Notch1 and IKKα signaling, which plays an essential role in inflammation, exacerbates the proliferation and inhibits the apoptosis in HT29 and other cell lines (128). Nevertheless, it has been reported that the blockage of Notch1 cascade has a protective effect toward CRC development in the ApcMin/+ mouse model of FAP (74). More recently, an elegant study from Taniguchi et al. showed that the co-receptor of IL-6 gp130 induces the activation of Notch1 without involving the classic gp130 effector STAT3, thus stimulating the cellular proliferation (83). However, the involvement of Notch1 pathway in intestinal cancer-related inflammation still represents a certain enigma. Indeed, our group has recently found that Notch1 signaling is down-regulated in the azoxymethane-dextran sodium sulfate (AOM-DSS) model of CAC, probably as effect of the epithelial damage due to DSS administration (114). Accordingly, Kim et al. have shown that the induced activation of Notch in the ApcMin/+ mouse model converted intestinal high-grade adenoma into low-grade adenoma, indicating a negative effect on cancer progression; they further demonstrated that this mechanism is mediated by the negative control of NRARP on WNT target genes (72). The involvement of β-catenin in concomitance to the protective role of Notch has been demonstrated also in our *in vivo* model of colitis-associated cancer (CAC), suggesting that these pathways (Notch and WNT) cooperate also under a certain setting of inflammatory conditions (114). Intriguingly, these opposing effects of inflammation on Notch1 signaling might underlie different mechanisms through which inflammation drives cancer development during sporadic CRC and CAC.

Then, the present work shows that CM is able to enhance the EMT in CRC cells, in particular regulating ZEB1 and MMP9 both at a protein and RNA level. Interestingly, Chanrion and colleagues found that the activation of Notch1 and the concomitant p53 deletion triggered EMT in the mouse gut (129); however, since HCT116 and HT29 have respectively wild type and mutant p53, we hypothesize that, in our model, the inflammation-driven EMT mechanism does not depend on p53. Even though it is well established that Notch1 signaling can be involved in the induction of EMT (92), less is known about the possible role of EMT as activator of Notch1. Noteworthy, in this study we demonstrate that inflammation induces the MMP9 overexpression and, as a consequence, the activation of the Notch1 pathway occurs. Accordingly, several reports acknowledge the tumorigenic role of MMP9 on Notch signaling pathway. For instance, it has been recently reported that the up-regulation of MMP9, linked to the activity of the protein Claudin-1, induces the Notch signaling activation, leading to the decrease of goblet cell number and thus enhancing the susceptibility to mucosal inflammation in the DSS-induced mouse model of colitis (84). Intriguingly, Garg and his group has recently shown that MMP9 up-regulation results in augmented levels of NICD in the AOM/DSS mouse model of CAC, but they attribute a protective role to this mechanism, in accordance with our previous results of Notch1 signaling in AOM-DSS treated mice (80). In contrast, as already discussed, the present study could mimic the effect of the inflammatory *milieu* on sporadic CRC, which deeply differs from the pro-inflammatory stimulus involved in CAC, probably explaining these opposite results.

In the last decades, Omega-3 polyunsaturated fatty acids (ω-3 PUFAs), and in particular the Eicosapentaenoic Acid (EPA), have been extensively studied for their possible role in the prevention and treatment of both inflammatory diseases and cancer (130). Indeed, it has been demonstrated that EPA is able to modulate several molecular pathways (110). One of the best characterized mechanisms of action is based on the capability of EPA to competing with the Arachidonic Acid, which is the substrate for the enzymatic action of COX-2; in this way, EPA

induces the reduction of the proinflammatory Prostaglandin of the series E2 in favour of the anti-inflammatory series E3 (131). Recently, we also demonstrated that the dietary supplementation of EPA, used as a free fatty acid in an extra pure formula with a higher level of bioavailability (EPA-FFA), significantly protected from cachexia and dramatically suppressed polyp number, size and burden in ApcMin/+ mice, by inhibiting COX-2 expression. Moreover, we showed that in the ApcMin/+ EPA-FFA was able to reduced β-catenin nuclear translocation, cell proliferation, and to induce an increase in apoptosis (113). Nevertheless, we recently found that EPA-FFA can also modulate the microbiota profile in the AOM/DSS mouse model (114). These findings suggest that EPA-FFA could regulate many unknown molecular pathways. Therefore, in the present model of inflammatory-driven CRC, we performed a prolonged pre-treatment with EPA-FFA both for 72h or 14 days on HT29 and HCT116 cells. We found that the incorporation of EPA into the cellular membrane was similar in these conditions, indicating that the maximum incorporation was reached very quickly, probably due to the FFA formulation. Importantly, our data show for the first time that EPA-FFA is able to hamper the CM-driven up-regulation of NICD and JAG1 in CRC cells and tends to inhibit the MMP9 activity in HCT116. Also, EPA-FFA counteracts the CM-induced cellular invasiveness in both cell lines, whereas HCT116 cells are known to exhibit higher invasion capability than HT29 cells (132). Similarly, Cheng-Chung Li and his group found that a treatment with EPA and DHA decreased MMP9 level in prostate cancer cells (133). It is important to note that, although the above-mentioned differences between our previous AOM-DSS *in vivo* work and the present *in vitro* study, EPA-FFA showed the same capability to modulate Notch1 signaling in both models (114).

In conclusion, we demonstrate for the first time that inflammation, inducing the MMP9 overexpression, strongly activates the Notch1 pathway and that this mechanism could be prevented by EPA-FFA in CRC.

6. BIBLIOGRAPHY

1. DiSario JA, Burt RW, Kendrick ML, McWhorter WP. Colorectal cancers of rare histologic types compared with adenocarcinomas. Dis Colon Rectum. 1994;37:1277–80.

2. Torre LA, Bray F, Siegel RL, Ferlay J, Lortet-Tieulent J, Jemal A. Global cancer statistics, 2012. CA Cancer J Clin. 2015;65:87–108.

3. Jemal A, Bray F, Center MM, Ferlay J, Ward E, Forman D. Global cancer statistics. CA Cancer J Clin. 61:69–90.

4. Haggar FA, Boushey RP. Colorectal cancer epidemiology: incidence, mortality, survival, and risk factors. Clin Colon Rectal Surg. 2009;22:191–7.

5. Huxley RR, Ansary-Moghaddam A, Clifton P, Czernichow S, Parr CL, Woodward M. The impact of dietary and lifestyle risk factors on risk of colorectal cancer: A quantitative overview of the epidemiological evidence. Int J Cancer. 2009;125:171–80.

6. Colussi D, Brandi G, Bazzoli F, Ricciardiello L. Molecular pathways involved in colorectal cancer: implications for disease behavior and prevention. Int J Mol Sci. 2013;14:16365–85.

7. Burt RW. Colon cancer screening. Gastroenterology. Elsevier; 2000;119:837–53.

8. Bach SP, Renehan AG, Potten CS. Stem cells: the intestinal stem cell as a paradigm. Carcinogenesis. 2000;21:469–76.

9. Fearon ER, Vogelstein B. A genetic model for colorectal tumorigenesis. Cell. 1990;61:759–67.

10. Wasan HS, Park H-S, Liu KC, Mandir NK, Winnett A, Sasieni P, et al. APC in the regulation of intestinal crypt fission. J Pathol. 1998;185:246–55.

11. Vogelstein B, Lane D, Levine AJ. Surfing the p53 network. Nature. 2000;408:307–10.

12. Guruswamy S, Rao C V. Multi-Target Approaches in Colon Cancer Chemoprevention Based on Systems Biology of Tumor Cell-Signaling. Gene Regul Syst Bio. 2008;2:163–76.

13. Smith G, Bounds R, Wolf H, Steele RJC, Carey FA, Wolf CR. Activating K-Ras mutations outwith “hotspot” codons in sporadic colorectal tumours - implications for personalised cancer medicine. Br J Cancer. 2010;102:693–703.

14. Leslie A, Carey FA, Pratt NR, Steele RJC. The colorectal adenoma-carcinoma sequence. Br J Surg. 2002;89:845–60.

15. Kinzler KW, Vogelstein B. Lessons from hereditary colorectal cancer. Cell. 1996;87:159–70.

16. Clevers H, Nusse R. Wnt/β-catenin signaling and disease. Cell. 2012;149:1192–205.

17. Worthley DL, Leggett BA. Colorectal cancer: molecular features and clinical opportunities. Clin Biochem Rev. 2010;31:31–8.

18. Bakhoum SF, Compton DA. Chromosomal instability and cancer: a complex relationship with therapeutic potential. J Clin Invest. American Society for Clinical Investigation; 2012;122:1138–43.

19. Toyota M, Ahuja N, Ohe-Toyota M, Herman JG, Baylin SB, Issa J-PJ. CpG island methylator phenotype in colorectal cancer. Proc Natl Acad Sci. 1999;96:8681–6.

20. Poulogiannis G, Frayling IM, Arends MJ. DNA mismatch repair deficiency in sporadic colorectal cancer and Lynch syndrome. Histopathology. 2010;56:167–79.

21. Dickinson BT, Kisiel J, Ahlquist DA, Grady WM. Molecular markers for colorectal cancer screening. Gut. 2015;64:1485–94.

22. Pancione M, Remo A, Colantuoni V. Genetic and epigenetic events generate multiple pathways in colorectal cancer progression. Patholog Res Int. 2012;2012:509348.

23. Jasperson KW, Tuohy TM, Neklason DW, Burt RW. Hereditary and familial colon cancer. Gastroenterology. 2010;138:2044–58.

24. Burt R, Neklason DW. Genetic testing for inherited colon cancer. Gastroenterology. 2005;128:1696–716.

25. Allen BA, Terdiman JP. Hereditary polyposis syndromes and hereditary non-polyposis colorectal cancer. Best Pract Res Clin Gastroenterol. 2003;17:237–58.

26. Valle L, Hernández-Illán E, Bellido F, Aiza G, Castillejo A, Castillejo M-I, et al. New insights into POLE and POLD1 germline mutations in familial colorectal cancer and polyposis. Hum Mol Genet. 2014;23:3506–12.

27. Groden J, Thliveris A, Samowitz W, Carlson M, Gelbert L, Albertsen H, et al. Identification and characterization of the familial adenomatous polyposis coli gene. Cell. 1991;66:589–600.

28. Goodenberger M, Lindor NM. Lynch syndrome and MYH-associated polyposis: review and testing strategy. J Clin Gastroenterol. 2011;45:488–500.

29. Terzić J, Grivennikov S, Karin E, Karin M. Inflammation and colon cancer. Gastroenterology. 2010;138:2101–14.e5.

30. Mattar MC, Lough D, Pishvaian MJ, Charabaty A. Current management of inflammatory bowel disease and colorectal cancer. Gastrointest Cancer Res. 2011;4:53–61.

31. Ullman TA, Itzkowitz SH. Intestinal inflammation and cancer. Gastroenterology. 2011;140:1807–16.

32. Waldner MJ, Neurath MF. Mechanisms of Immune Signaling in Colitis-Associated Cancer. C Cell Mol Gastroenterol Hepatol. 2015;1:6–16.

33. Olaru A V, Cheng Y, Agarwal R, Yang J, David S, Abraham JM, et al. Unique patterns of CpG island methylation in inflammatory bowel disease-associated colorectal cancers. Inflamm Bowel Dis. 2012;18:641–8.

34. Aust DE, Terdiman JP, Willenbucher RF, Chang CG, Molinaro-Clark A, Baretton GB, et al. The APC/beta-catenin pathway in ulcerative colitis-related colorectal carcinomas: a mutational analysis. Cancer. 2002;94:1421–7.

35. Hussain SP, Amstad P, Raja K, Ambs S, Nagashima M, Bennett WP, et al. Increased p53 Mutation Load in Noncancerous Colon Tissue from Ulcerative Colitis: A Cancer-prone Chronic Inflammatory Disease. Cancer Res. 2000;60:3333–7.

36. Issa J-PJ, Ahuja N, Toyota M, Bronner MP, Brentnall TA. Accelerated Age-related CpG Island Methylation in Ulcerative Colitis. Cancer Res. 2001;61:3573–7.

37. Fleisher AS, Esteller M, Harpaz N, Leytin A, Rashid A, Xu Y, et al. Microsatellite instability in inflammatory bowel disease-associated neoplastic lesions is associated with hypermethylation and diminished expression of the DNA mismatch repair gene, hMLH1. Cancer Res. 2000;60:4864–8.

38. Cancers Complicating Inflammatory Bowel Disease - NEJMra1403718 [Internet]. [cited 2016 Jan 25]. Available from: http://www.nejm.org/doi/pdf/10.1056/NEJMra1403718

39. Dyson JK, Rutter MD. Colorectal cancer in inflammatory bowel disease: what is the real magnitude of the risk? World J Gastroenterol. 2012;18:3839–48.

40. Burnett-Hartman AN, Newcomb PA, Potter JD. Infectious agents and colorectal cancer: a review of Helicobacter pylori, Streptococcus bovis, JC virus, and human papillomavirus. Cancer Epidemiol Biomarkers Prev. 2008;17:2970–9.

41. Irrazábal T, Belcheva A, Girardin SE, Martin A, Philpott DJ. The Multifaceted Role of the Intestinal Microbiota in Colon Cancer. Mol Cell. 2014;54:309–20.

42. Bardou M, Barkun AN, Martel M. Obesity and colorectal cancer. Gut. 2013;62:933–47.

43. Mantovani A, Allavena P, Sica A, Balkwill F. Cancer-related inflammation. Nature. 2008;454:436–44.

44. Colotta F, Allavena P, Sica A, Garlanda C, Mantovani A. Cancer-related inflammation, the seventh hallmark of cancer: links to genetic instability. Carcinogenesis. 2009;30:1073–81.

45. Mantovani A, Allavena P, Sica A, Balkwill F. Cancer-related inflammation. Nature. Nature Publishing Group; 2008;454:436–44.

46. Sheikh SZ, Plevy SE. The role of the macrophage in sentinel responses in intestinal immunity. Curr Opin Gastroenterol. 2010;26:578–82.

47. Erreni M, Mantovani A, Allavena P. Tumor-associated Macrophages (TAM) and Inflammation in Colorectal Cancer. Cancer Microenviron. 2011;4:141–54.

48. Inflammation and Colon Cancer - gastro1.pdf [Internet]. [cited 2016 Jan 25]. Available from: http://journalsconsultapp.elsevier-eprints.com/uploads/articles/gastro1.pdf

49. Yu H, Kortylewski M, Pardoll D. Crosstalk between cancer and immune cells: role of STAT3 in the tumour microenvironment. Nat Rev Immunol. 2007;7:41–51.

50. Karin M. Nuclear factor-kappaB in cancer development and progression. Nature. 2006;441:431–6.

51. Lee YS, Choi I, Ning Y, Kim NY, Khatchadourian V, Yang D, et al. Interleukin-8 and its receptor CXCR2 in the tumour microenvironment promote colon cancer growth, progression and metastasis. Br J Cancer. 2012;106:1833–41.

52. Ning Y, Manegold PC, Hong YK, Zhang W, Pohl A, Lurje G, et al. Interleukin-8 is associated with proliferation, migration, angiogenesis and chemosensitivity in vitro and in vivo in colon cancer cell line models. Int J Cancer. 2011;128:2038–49.

53. Reissfelder C, Stamova S, Gossmann C, Braun M, Bonertz A, Walliczek U, et al. Tumor-specific cytotoxic T lymphocyte activity determines colorectal cancer patient prognosis. J Clin Invest. 2014;125:739–51.

54. Grivennikov SI, Karin M. Inflammation and oncogenesis: a vicious connection. Curr Opin Genet Dev. 2010;20:65–71.

55. Hori K, Sen A, Artavanis-Tsakonas S. Notch signaling at a glance. J Cell Sci. 2013;126:2135–40.

56. Bray SJ. Notch signalling: a simple pathway becomes complex. Nat Rev Mol Cell Biol. 2006;7:678–89.

57. Artavanis-Tsakonas S. Notch Signaling: Cell Fate Control and Signal Integration in Development. Science (80-). 1999;284:770–6.

58. Andersson ER, Sandberg R, Lendahl U. Notch signaling: simplicity in design, versatility in function. Development. 2011;138:3593–612.

59. Allenspach EJ, Maillard I, Aster JC, Pear WS. Notch signaling in cancer. Cancer Biol Ther. 1:466–76.

60. Rebay I, Fleming RJ, Fehon RG, Cherbas L, Cherbas P, Artavanis-Tsakonas S. Specific EGF repeats of Notch mediate interactions with Delta and Serrate: implications for Notch as a multifunctional receptor. Cell. 1991;67:687–99.

61. Kopan R, Ilagan MXG. The canonical Notch signaling pathway: unfolding the activation mechanism. Cell. 2009;137:216–33.

62. Yang L-T. Fringe Glycosyltransferases Differentially Modulate Notch1 Proteolysis Induced by Delta1 and Jagged1. Mol Biol Cell. 2004;16:927–42.

63. Guruharsha KG, Kankel MW, Artavanis-Tsakonas S. The Notch signalling system: recent insights into the complexity of a conserved pathway. Nat Rev Genet. Nature Publishing Group, a division of Macmillan Publishers Limited. All Rights Reserved.; 2012;13:654–66.

64. Guilmeau S. Notch signaling and intestinal cancer. Adv Exp Med Biol. 2012;727:272–88.

65. Ayaz F, Osborne BA. Non-canonical notch signaling in cancer and immunity. Front Oncol. 2014;4:345.

66. Miele L, Golde T, Osborne B. Notch signaling in cancer. Curr Mol Med. 2006;6:905–18.

67. Andersen P, Uosaki H, Shenje LT, Kwon C. Non-canonical Notch signaling: emerging role and mechanism. Trends Cell Biol. 2012;22:257–65.

68. Miyamoto S, Rosenberg DW. Role of Notch signaling in colon homeostasis and carcinogenesis. Cancer Sci. 2011;102:1938–42.

69. Ranganathan P, Weaver KL, Capobianco AJ. Notch signalling in solid tumours: a little bit of everything but not all the time. Nat Rev Cancer. Nature Publishing Group, a division of Macmillan Publishers Limited. All Rights Reserved.; 2011;11:338–51.

70. Pellegrinet L, Rodilla V, Liu Z, Chen S, Koch U, Espinosa L, et al. Dll1- and dll4-mediated notch signaling are required for homeostasis of intestinal stem cells. Gastroenterology. 2011;140:1230–40.e1–7.

71. Dai Y, Wilson G, Huang B, Peng M, Teng G, Zhang D, et al. Silencing of Jagged1 inhibits cell growth and invasion in colorectal cancer. Cell Death Dis. Macmillan Publishers Limited; 2014;5:e1170.

72. Kim H-A, Koo B-K, Cho J-H, Kim Y-Y, Seong J, Chang HJ, et al. Notch1 counteracts WNT/β-catenin signaling through chromatin modification in colorectal cancer. J Clin Invest. American Society for Clinical Investigation; 2012;122:3248–59.

73. Reedijk M, Odorcic S, Zhang H, Chetty R, Tennert C, Dickson BC, et al. Activation of Notch signaling in human colon adenocarcinoma. Int J Oncol. 2008;33:1223–9.

74. Van Es JH, van Gijn ME, Riccio O, van den Born M, Vooijs M, Begthel H, et al. Notch/gamma-secretase inhibition turns proliferative cells in intestinal crypts and adenomas into goblet cells. Nature. 2005;435:959–63.

75. Koch U, Radtke F. Notch and cancer: a double-edged sword. Cell Mol Life Sci. 2007;64:2746–62.

76. Zhang Q, Wang C, Liu Z, Liu X, Han C, Cao X, et al. Notch signal suppresses Toll-like receptor-triggered inflammatory responses in macrophages by inhibiting extracellular signal-regulated kinase 1/2-mediated nuclear factor κB activation. J Biol Chem. 2012;287:6208–17.

77. Espinosa L, Inglés-Esteve J, Robert-Moreno A, Bigas A. IkappaBalpha and p65 regulate the cytoplasmic shuttling of nuclear corepressors: cross-talk between Notch and NFkappaB pathways. Mol Biol Cell. 2003;14:491–502.

78. Zheng X, Linke S, Dias JM, Gradin K, Wallis TP, Hamilton BR, et al. Interaction with factor inhibiting HIF-1 defines an additional mode of cross-coupling between the Notch and hypoxia signaling pathways. Proc Natl Acad Sci. 2008;105:3368–73.

79. Timmerman LA, Grego-Bessa J, Raya A, Bertrán E, Pérez-Pomares JM, Díez J, et al. Notch promotes epithelial-mesenchymal transition during cardiac development and oncogenic transformation. Genes Dev. 2004;18:99–115.

80. Garg P, Sarma D, Jeppsson S, Patel NR, Gewirtz AT, Merlin D, et al. Matrix metalloproteinase-9 functions as a tumor suppressor in colitis-associated cancer. Cancer Res. 2010;70:792–801.

81. Liu Z-J, Xiao M, Balint K, Soma A, Pinnix CC, Capobianco AJ, et al. Inhibition of endothelial cell proliferation by Notch1 signaling is mediated by repressing MAPK and PI3K/Akt pathways and requires MAML1. FASEB J. 2006;20:1009–11.

82. Lin J-T, Wang J-Y, Chen M-K, Chen H-C, Chang T-H, Su B-W, et al. Colon cancer mesenchymal stem cells modulate the tumorigenicity of colon cancer through interleukin 6. Exp Cell Res. 2013;319:2216–29.

83. Taniguchi K, Wu L-W, Grivennikov SI, de Jong PR, Lian I, Yu F-X, et al. A gp130–Src–YAP module links inflammation to epithelial regeneration. Nature. 2015;519:57–62.

84. Pope JL, Bhat AA, Sharma A, Ahmad R, Krishnan M, Washington MK, et al. Claudin-1 regulates intestinal epithelial homeostasis through the modulation of Notch-signalling. Gut. 2014;63:622–34.

85. Kalluri R, Weinberg RA. The basics of epithelial-mesenchymal transition. J Clin Invest. 2009;119:1420–8.

86. Kalluri R, Weinberg RA. The basics of epithelial-mesenchymal transition. J Clin Invest. American Society for Clinical Investigation; 2009;119:1420–8.

87. Lamouille S, Xu J, Derynck R. Molecular mechanisms of epithelial-mesenchymal transition. Nat Rev Mol Cell Biol. 2014;15:178–96.

88. Grille SJ, Bellacosa A, Upson J, Klein-Szanto AJ, van Roy F, Lee-Kwon W, et al. The protein kinase Akt induces epithelial mesenchymal transition and promotes enhanced motility and invasiveness of squamous cell carcinoma lines. Cancer Res. 2003;63:2172–8.

89. Barrallo-Gimeno A. The Snail genes as inducers of cell movement and survival: implications in development and cancer. Development. 2005;132:3151–61.

90. Peinado H, Olmeda D, Cano A. Snail, Zeb and bHLH factors in tumour progression: an alliance against the epithelial phenotype? Nat Rev Cancer. 2007;7:415–28.

91. Lin C-Y, Tsai P-H, Kandaswami CC, Lee P-P, Huang C-J, Hwang J-J, et al. Matrix metalloproteinase-9 cooperates with transcription factor Snail to induce epithelial-mesenchymal transition. Cancer Sci. 2011;102:815–27.

92. Wang Z, Li Y, Kong D, Sarkar FH. The role of Notch signaling pathway in epithelial-mesenchymal transition (EMT) during development and tumor aggressiveness. Curr Drug Targets. 2010;11:745–51.

93. Sullivan NJ, Sasser AK, Axel AE, Vesuna F, Raman V, Ramirez N, et al. Interleukin-6 induces an epithelial-mesenchymal transition phenotype in human breast cancer cells. Oncogene. 2009;28:2940–7.

94. Fernando RI, Castillo MD, Litzinger M, Hamilton DH, Palena C. IL-8 signaling plays a critical role in the epithelial-mesenchymal transition of human carcinoma cells. Cancer Res. 2011;71:5296–306.

95. Tsai JH, Yang J. Epithelial-mesenchymal plasticity in carcinoma metastasis. Genes Dev. 2013;27:2192–206.

96. Moreno-Bueno G, Portillo F, Cano A. Transcriptional regulation of cell polarity in EMT and cancer. Oncogene. Macmillan Publishers Limited; 2008;27:6958–69.

97. Loboda A, Nebozhyn M V, Watters JW, Buser CA, Shaw P, Huang PS, et al. EMT is the dominant program in human colon cancer. BMC Med Genomics. 2011;4:9.

98. Kaur N, Chugh V, Gupta AK. Essential fatty acids as functional components of foods- a review. J Food Sci Technol. 2014;51:2289–303.

99. Lenihan-Geels G, Bishop K, Ferguson L. Alternative Sources of Omega-3 Fats: Can We Find a Sustainable Substitute for Fish? Nutrients. 2013;5:1301–15.

100. Rennison JH, Van Wagoner DR. Impact of dietary fatty acids on cardiac arrhythmogenesis. Circ Arrhythm Electrophysiol. 2009;2:460–9.

101. Siddiqui RA, Shaikh SR, Sech LA, Yount HR, Stillwell W, Zaloga GP. Omega 3-fatty acids: health benefits and cellular mechanisms of action. Mini Rev Med Chem. 2004;4:859–71.

102. Hull MA. Omega-3 polyunsaturated fatty acids. Best Pract Res Clin Gastroenterol. 2011;25:547–54.

103. Tapiero H, Ba GN, Couvreur P, Tew KD. Polyunsaturated fatty acids (PUFA) and eicosanoids in human health and pathologies. Biomed Pharmacother = Biomédecine pharmacothérapie. 2002;56:215–22.

104. Kohli P, Levy BD. Resolvins and protectins: mediating solutions to inflammation. Br J Pharmacol. 2009;158:960–71.

105. Hudert CA, Weylandt KH, Lu Y, Wang J, Hong S, Dignass A, et al. Transgenic mice rich in endogenous omega-3 fatty acids are protected from colitis. Proc Natl Acad Sci U S A. 2006;103:11276–81.

106. Zhang P, Smith R, Chapkin RS, McMurray DN. Dietary (n-3) Polyunsaturated Fatty Acids Modulate Murine Th1/Th2 Balance toward the Th2 Pole by Suppression of Th1 Development. J Nutr. 2005;135:1745–51.

107. Oh DY, Olefsky JM. Omega 3 Fatty Acids and GPR120. Cell Metab. 2012;15:564–5.

108. Turk HF, Chapkin RS. Membrane lipid raft organization is uniquely modified by n-3 polyunsaturated fatty acids. Prostaglandins, Leukot Essent Fat Acids. 2013;88:43–7.

109. Kantor ED, Lampe JW, Peters U, Vaughan TL, White E. Long-Chain Omega-3 Polyunsaturated Fatty Acid Intake and Risk of Colorectal Cancer. Nutr Cancer. 2013;

110. Cockbain AJ, Toogood GJ, Hull MA. Omega-3 polyunsaturated fatty acids for the treatment and prevention of colorectal cancer. Gut. 2012;61:135–49.

111. Cockbain AJ, Volpato M, Race AD, Munarini A, Fazio C, Belluzzi A, et al. Anticolorectal cancer activity of the omega-3 polyunsaturated fatty acid eicosapentaenoic acid. Gut. 2014;

112. West NJ, Clark SK, Phillips RKS, Hutchinson JM, Leicester RJ, Belluzzi A, et al. Eicosapentaenoic acid reduces rectal polyp number and size in familial adenomatous polyposis. Gut. 2010;59:918–25.

113. Fini L, Piazzi G, Ceccarelli C, Daoud Y, Belluzzi A, Munarini A, et al. Highly purified eicosapentaenoic acid as free fatty acids strongly suppresses polyps in Apc(Min/+) mice. Clin Cancer Res. 2010;16:5703–11.

114. Piazzi G, D'Argenio G, Prossomariti A, Lembo V, Mazzone G, Candela M, et al. Eicosapentaenoic acid free fatty acid prevents and suppresses colonic neoplasia in colitis-associated colorectal cancer acting on Notch signaling and gut microbiota. Int J Cancer. 2014;

115. Park EK, Jung HS, Yang HI, Yoo MC, Kim C, Kim KS. Optimized THP-1 differentiation is required for the detection of responses to weak stimuli. Inflamm Res. 2007;56:45–50.

116. Daigneault M, Preston JA, Marriott HM, Whyte MKB, Dockrell DH. The identification of markers of macrophage differentiation in PMA-stimulated THP-1 cells and monocyte-derived macrophages. PLoS One. 2010;5:e8668.

117. Brummelkamp TR, Bernards R, Agami R. A system for stable expression of short interfering RNAs in mammalian cells. Science. 2002;296:550–3.

118. Albini A, Benelli R. The chemoinvasion assay: a method to assess tumor and endothelial cell invasion and its modulation. Nat Protoc. Nature Publishing Group; 2007;2:504–11.

119. Sansone P, Piazzi G, Paterini P, Strillacci A, Ceccarelli C, Minni F, et al. Cyclooxygenase-2/carbonic anhydrase-IX up-regulation promotes invasive potential and hypoxia survival in colorectal cancer cells. J Cell Mol Med. Wiley-Blackwell; 2009;13:3876–87.

120. Yang J, Zhang L, Yu C, Yang X-F, Wang H. Monocyte and macrophage differentiation: circulation inflammatory monocyte as biomarker for inflammatory diseases. Biomark Res. 2014;2:1.

121. Valledor AF, Borràs FE, Cullell-Young M, Celada A. Transcription factors that regulate monocyte/macrophage differentiation. J Leukoc Biol. 1998;63:405–17.

122. Takashiba S, Van Dyke TE, Amar S, Murayama Y, Soskolne AW, Shapira L. Differentiation of monocytes to macrophages primes cells for lipopolysaccharide stimulation via accumulation of cytoplasmic nuclear factor kappaB. Infect Immun. 1999;67:5573–8.

123. Hwang W-L, Yang M-H, Tsai M-L, Lan H-Y, Su S-H, Chang S-C, et al. SNAIL regulates interleukin-8 expression, stem cell-like activity, and tumorigenicity of human colorectal carcinoma cells. Gastroenterology. 2011;141:279–91, 291.e1–5.

124. Wang H, Wang H-S, Zhou B-H, Li C-L, Zhang F, Wang X-F, et al. Epithelial-mesenchymal transition (EMT) induced by TNF-α requires AKT/GSK-3β-mediated stabilization of snail in colorectal cancer. PLoS One. 2013;8:e56664.

125. Palena C, Hamilton DH, Fernando RI. Influence of IL-8 on the epithelial-mesenchymal transition and the tumor microenvironment. Future Oncol. 2012;8:713–22.

126. De Simone V, Franzè E, Ronchetti G, Colantoni A, Fantini MC, Di Fusco D, et al. Th17-type cytokines, IL-6 and TNF-α synergistically activate STAT3 and NF-kB to promote colorectal cancer cell growth. Oncogene. 2014;

127. Peignon G, Durand A, Cacheux W, Ayrault O, Terris B, Laurent-Puig P, et al. Complex interplay between β-catenin signalling and Notch effectors in intestinal tumorigenesis. Gut. 2011;60:166–76.

128. Fernández-Majada V, Aguilera C, Villanueva A, Vilardell F, Robert-Moreno A, Aytés A, et al. Nuclear IKK activity leads to dysregulated notch-dependent gene expression in colorectal cancer. Proc Natl Acad Sci U S A. 2007;104:276–81.

129. Chanrion M, Kuperstein I, Barrière C, El Marjou F, Cohen D, Vignjevic D, et al. Concomitant Notch activation and p53 deletion trigger epithelial-to-mesenchymal transition and metastasis in mouse gut. Nat Commun. Nature Publishing Group; 2014;5:5005.

130. Wall R, Ross RP, Fitzgerald GF, Stanton C. Fatty acids from fish: the anti-inflammatory potential of long-chain omega-3 fatty acids. Nutr Rev. 2010;68:280–9.

131. Hawcroft G, Loadman PM, Belluzzi A, Hull MA. Effect of eicosapentaenoic acid on E-type prostaglandin synthesis and EP4 receptor signaling in human colorectal cancer cells. Neoplasia. 2010;12:618–27.

132. Liu Y, Zhang F, Zhang X-F, Qi L-S, Yang L, Guo H, et al. Expression of nucleophosmin/NPM1 correlates with migration and invasiveness of colon cancer cells. J Biomed Sci. 2012;19:53.

133. Li C-C, Hou Y-C, Yeh C-L, Yeh S-L. Effects of eicosapentaenoic acid and docosahexaenoic acid on prostate cancer cell migration and invasion induced by tumor-associated macrophages. PLoS One. 2014;9:e99630.